High Dub3 expression in mouse ESC couples the G1/S checkpoint to pluripotency

Siem van Der Laan, Nicolay Tsanov, Carole Crozet, Domenico Maiorano

High Dub3 expression in mouse ES cells couples the G1/S checkpoint to pluripotency

Siem VAN DER LAAN[1], Nikolay TSANOV[1,2], Carole CROZET[3] and Domenico MAIORANO[1*]

[1]Genome Surveillance and Stability laboratory
[3]Neurological Disorders and Stem Cells
CNRS-UPR1142, Institute of Human Genetics
141, rue de la cardonille. 34396 Cedex 5. Montpellier
FRANCE

*Contact
Email: domenico.maiorano@igh.cnrs.fr
Tel.: +33(0)434359973
Fax: +33(0)434359901

[2] Present address: Institute of Molecular Genetics. Laboratory of RNA biogenesis. 1919 route de mende. Montpellier Cedex
[3] Present address: Institut de Recherche en Biothérapies. 80, av. Augustin Fliche 34295 Montpellier Cedex 5

Keywords: DNA damage - Cdc25A - Esrrb - cell cycle - development
Running title: Dub3-Cdc25A and checkpoint bypass in ES cells

Summary

The molecular mechanism underlying G1/S checkpoint bypass in mouse embryonic stem (ES) cells remains unknown. DNA damage blocks S-phase entry by inhibiting the CDK2 kinase through destruction of its activator, the Cdc25A phosphatase. We observed high Cdc25A levels in G1 that persist even after DNA damage in mouse ES cells. We also found higher expression of Dub3, a deubiquitylase that controls Cdc25A protein abundance. Moreover, we demonstrate that the Dub3 gene is a direct target of Esrrb, a key transcription factor of the self-renewal machinery. We show that Dub3 expression is strongly downregulated during neural conversion and precedes Cdc25A destabilization, while forced Dub3 expression in ES cells becomes lethal upon differentiation, concomitant to cell cycle remodelling and lineage commitment. Finally, knockdown of either Dub3 or Cdc25A induced spontaneous differentiation of ES cells. Altogether, these findings couple the self-renewal machinery to cell cycle control through a deubiquitylase in ES cells.

Highlights (85 character per point)

- Cdc25A persistence upon DNA damage sustains G1/S checkpoint bypass in ES cells
- Dub3 is rapidly downregulated during neural conversion and Cdc25A is destabilized
- Dub3 is a target of Esrrb, a key transcription factor of the self-renewal machinery
- Dub3 or Cdc25A knockdown induces heterogeneous differentiation in the presence of LIF

Introduction

Eukaryotic cells have developed checkpoints to block cell cycle progression upon DNA damage or replication stress (Ciccia and Elledge, 2010). Two distinct pathways pertain to the G1/S checkpoint by directly reducing CDK2 activity: *a)* rapid destruction of the Cdc25A phosphatase resulting in increased CDK2 phosphorylation (Mailand et al., 2000; Sexl et al., 1999), and *b)* a slower, p53-mediated, transcriptional response that activates expression of, amongst others, the potent CDK2 inhibitor p21 (Brugarolas et al., 1995; Dulic et al., 1994). Importantly, rapid p21 degradation observed after exposure to low UV doses may be important for optimal DNA repair (Bendjennat et al., 2003; Chen et al., 2004; Lee et al., 2006), while inhibition of CDK2 activity following Cdc25A degradation is sufficient for cell cycle arrest (Bendjennat et al., 2003). Cdc25A protein levels are tightly regulated by two E3 ubiquitin ligases, the Anaphase Promoting Complex/Cyclosome (APC/C^{Cdh1}) as cells exit mitosis, and the Skp1-Cullin1-Fbox ($SCF^{\beta-TrCP}$) during both S and G2 phase and following DNA damage (Busino et al., 2003; Donzelli et al., 2002).

Compared to somatic cells, mouse embryonic stem (ES) cells appear to have a relaxed G1/S checkpoint (Aladjem et al., 1998; Hong and Stambrook, 2004; Koledova et al., 2010; Prost et al., 1998). The molecular mechanism underlying this feature remains unclear. Moreover, mouse ES cell cycle has remarkably short G1 and G2 phases, with little S phase length variation (Ballabeni et al., 2011; Savatier et al., 2002; White et al., 2005). This is underpinned by high CDK2/Cyclin E activity (Stead et al., 2002) and reduced APC/C activity leading to limited oscillation in substrate levels (Ballabeni et al., 2011). Interestingly, knockdown of CDK2 protein was shown to increase G1 length although DNA damage-dependent degradation of Cdc25A was reported not to affect CDK2 activity, nor to induce a G1 arrest

(Koledova et al., 2010; Neganova et al., 2011; Neganova et al., 2009). In contrast, a previous study reported that Cdc25A is not degraded upon γ-irradiation in ES cells (Hong and Stambrook, 2004).

Maintenance of pluripotency depends upon expression of pluripotency genes under the combinatorial control of a regulatory network of transcription factors such as Nanog, Sox2 and Oct4 (Festuccia et al., 2013; van den Berg et al., 2008). Differentiation of ES cell induces cell cycle remodelling, including appearance of longer G1 and G2 phases, but how this regulation is achieved is unknown. Moreover, how the pluripotency regulatory network impacts onto cell cycle control remains obscure. Aside from its well-known role in somatic cell cycle, very little is known about Cdc25A function in ES cells. In human ES cells, Cdc25A expression was shown to be regulated by Nanog (Zhang et al., 2009). A recent report shows that Nanog knockdown in mouse ES cells results in G1/S transition delay by an unknown mechanism (Chen et al., 2012). Equally, the role of p53 in ES cells G1/S DNA damage checkpoint still remains controversial (Aladjem et al., 1998; Sabapathy et al., 1997; Solozobova et al., 2009). Despite its high abundance, p53 has been proposed to be inactive in ES cells due to a predominant cytoplasmic distribution (Solozobova et al., 2009).

In this study we sought to understand the molecular grounds for inefficient G1/S DNA damage checkpoint in ES cells. We found that high Cdc25A abundance sustains G1/S checkpoint bypass in ES cells. We show that Cdc25A abundance depends upon high expression of Dub3, a deubiquitylase that fine-tunes Cdc25A steady-state levels (Pereg et al., 2010). Moreover, we identify Dub3 as a novel target gene of estrogen-related-receptor-b (Esrrb), a key transcription factor of the self-renewal machinery (Festuccia et al., 2012; Ivanova et al., 2006; Martello et al., 2012).

Strikingly, we observed acute downregulation of Dub3 expression upon differentiation and its knockdown induced spontaneous ES cell differentiation. In sum, our data interconnect the self-renewal machinery to cell cycle control and highlight the importance of deubiquitylases in stem cell and developmental biology.

Results

ES cells arrest in early S phase upon induction of DNA damage in G1

Circumstantial data suggest an impaired G1/S checkpoint in ES cells (Hong and Stambrook, 2004; Koledova et al., 2010; Aladjem et al., 1998; Prost et al., 1998). We observed that irradiation of ES cells with increasing doses of UV light induced a decrease in the number of G1 cells (Figure S1A). Time course analysis with a single UV dose (6 J/m^2) resulted in cell cycle delay at the G1/S boundary (Figure S1B, t=2). We pulse-labelled nocodazole synchronized cells with BrdU (a nucleotide analogue) to allow exact distinction between late G1 (BrdU-negative) and early S-phase (BrdU-positive, Figure 1A). While analysis of total DNA content suggests a G1 arrest (Figure 1B), analysis of BrdU incorporation revealed that both untreated (Mock) and UV-irradiated cells (+ UV) entered S phase with very similar kinetics (Figure 1C-D). In contrast, synchronized mouse embryonic fibroblasts (NIH-3t3), which are Oct4-negative differentiated cells (Figure S1C), did not progress to S phase after UV irradiation in G1 (Figure 1E), in line with the presence of a stringent G1/S checkpoint.

We noticed that upon UV irradiation, BrdU incorporation was slightly reduced compared to mock-irradiated cells, confirmed by calculating the mean fluorescent signal of BrdU-positive cells (Figure 1E, green boxes), and suggesting DNA synthesis slowdown in very early S phase. Analysis of chromatin-bound proteins shows that recruitment of both Cdc45 and DNA polymerase-α, two replication fork-associated factors, was considerably reduced upon UV irradiation, but not abolished (Figure S1D, compare lanes 2-4 with 5-7), suggesting activation of the S phase checkpoint preventing late replication origins firing (Karnani and Dutta, 2011). Consistent with this possibility, phosphorylated H2AX histone variant (γH2AX), an ATR substrate, accumulated onto chromatin. Moreover UV-induced DNA damage did

not significantly change the transcriptional program driven by E2F transcription factors required for S phase entry, as monitored by Cyclin A2 and E1 production (Figure S1E). We also observed UV damage-dependent p53 phosphorylation on chromatin (Figure S2A), and transactivation (amongst other) of p21 gene expression (Figure S2B-D), demonstrating a functional p53 transcriptional response, in line with a previous study (Solozobova et al., 2009).

Persistent high levels of Cdc25A in ES cells sustain G1/S checkpoint bypass

Cdc25A functions as a critical CDK2 regulator by removing an inhibitory phosphorylation on Tyrosine 15 ($CDK2^{Y15P}$) that in turn regulates S phase progression. We compared Cdc25A and CDK2 protein abundance between ES cells and NIH-3t3 cells (Figure 2A). Strikingly, while CDK2 abundance is marginally higher in ES cells, the levels of Cdc25A in asynchronously growing ES cells are exceedingly high compared to NIH-3t3 cells. As expected, upon UV-induced DNA damage, Cdc25A was degraded in both cell lines (Figure 2A). However, one hour after irradiation, Cdc25A level remained about 4-fold higher in ES cells compared to unperturbed NIH-3t3 cells (lanes 1 and 7 and Figure S3A), indicating that high levels of Cdc25A persist even upon UV-induced DNA damage. Since cell cycle distribution of asynchronously growing ES and NIH-3t3 cells is different, we analysed Cdc25A abundance in synchronized cells (Figure 2B). We observed that in G1, ES cells contained about 7-fold more Cdc25A protein than NIH-3t3 cells (lanes 3 and 11 and Figure S3B). Proteolysis of Cdc25A mediated by the E3 ubiquitin ligase APC^{Cdh1} occurs at mitotic exit (Donzelli et al., 2002). Polyubiquitylated forms appear as a polypeptide ladder of higher molecular weight than the unmodified protein. In NIH-3t3 cells synchronized in G1 and S phase, we could observe such ladders by western

blot using a specific Cdc25A antibody (Figure 2B, dark). Strikingly, in synchronized ES cells, these isoforms are much less abundant, whereas levels of unmodified Cdc25A are 7-fold higher than in NIH-3t3 cells (Figure S3B). Cdc25A immunoprecipitation from either ES or NIH-3t3 cells cotransfected with GFP-Cdc25A and HA-tagged ubiquitin, confirmed the presence of much more Cdc25A polyubiquitylated forms in NIH-3t3 than in ES cells (Figure 2C), corroborating recent data (Buckley et al., 2012).

Next we tested whether incomplete Cdc25A degradation may be due to impaired function of the ATR-Chk1 pathway. To this end, we treated cells with a Chk1 inhibitor and analyzed Cdc25A protein levels upon UV irradiation. In contrast to a previous report in which degradation of Cdc25A was not affected by both Chk1 and Chk2 inhibitors (Koledova et al., 2010), we observed that Cdc25A degradation in ES cells is entirely dependent on Chk1 activity (Figure 2D). One explanation for this discrepancy may be that we analysed Cdc25A protein turnover in presence of cycloheximide to inhibit translation, since it is known that Cdc25A abundance is also regulated at this level (Gautier et al., 2012).

Treatment of asynchronously growing ES cells with roscovitine (a selective CDKs inhibitor) induced dose-dependent increase of G1 cells and reduced the fraction of S phase cells (Figure S3C), demonstrating that, similar to somatic cells, in ES cells CDK activity is necessary for the G1/S transition. Inhibitory CDK2^{Y15} phosphorylation is mediated by Wee1 kinase and relieved through dephosphorylation by Cdc25A (Busino et al., 2004; Malumbres and Barbacid, 2001). We therefore analysed changes in protein level of Wee1, Cdc25A, and CDK2^{Y15P} during G1/S transition in ES cells, which, according to BrdU uptake experiments, occurs between 2-3 hours after nocodazole release (Figure 1C). Mitotic exit was monitored by histone

H3 phosphorylation at serine 10 ($H3^{S10P}$), and S phase entry by H3 and Cyclin A production. Interestingly, Wee1 levels did not show significant cell cycle-dependent variations, while Cdc25A levels decreased and inversely correlated with $CDK2^{Y15P}$ abundance (Figure S3D-E), suggesting that in ES cells, cell cycle-dependent fluctuation of Cdc25A levels may specifically regulate $CDK2^{Y15P}$.

To further pinpoint the specific role of Cdc25A in the G1/S checkpoint, we examined whether interfering with Cdc25A levels by RNAi affects S-phase entry upon DNA damage (Figure S3F-G). To avoid undesired differentiation of ES cells due to G1 phase extension upon Cdc25A downregulation that would interfere with the interpretation of this experiment (see below and Figure 6E-F), knockdown was performed over a short period (24 hours). Interestingly, Cdc25A knockdown (Figure 2E) resulted in a significant, UV-dependent, increase of BrdU-negative cells with 2N DNA content (Figure 2F) mirrored by increased $CDK2^{Y15P}$ levels (Figure 2E, compare lane 3 with lane 6 and Figure S3H). Importantly, the slight increase of $CDK2^{Y15P}$ levels between 2 and 4 hours after release (Figure 2E, lane 3), also observed in synchronized undamaged cells entering S-phase (Figure S3D), did not result in an apparent difference in S phase entry in mock and UV-treated cells transfected with control RNAi (Figure 2F). Altogether, these data show that ES cells contain high levels of Cdc25A and that its knockdown leads to a UV-dependent G1 delay.

ES cells express high Dub3 deubiquitylase

Elevated Cdc25A protein levels can be explained by increased gene expression, increased translation or reduced protein degradation. We analysed protein turnover in the presence of cycloheximide to inhibit *de novo* protein synthesis (Figure S4A-B).

Using this approach, we found a 3-fold longer half-life of Cdc25A in ES cells ($t_{1/2}$= 24 min) compared to NIH-3t3 cells ($t_{1/2}$= 8 min). Of note, since unsynchronized cells were used, we cannot exclude that the observed difference is partly due to distinct cell cycle distribution of both cell types. However, this data strongly suggests alterations in protein stability that, according to data shown in Figure 2B-C, might reflect differences between polyubiquitylation and ubiquitin removal by hydrolysation (deubiquitylation). To address this point, we compared gene expression of Cdc25A, Cdh1, β-TrCP and that of the recently described Dub3 deubiquitylase (Pereg et al., 2010), between ES and NIH-3t3 cells. Whereas mRNA levels of Cdc25A, Cdh1 and β–TrCP in ES cells hardly differ from NIH-3t3 cells, Dub3 mRNA level was 4-fold higher in ES cells (Figure 3A). Moreover, RNAi-mediated knockdown of Dub3 in ES cells (Figure 3B) did not affect Cdc25A mRNA level (Figure 3C) but resulted in 3-fold reduction of Cdc25A protein abundance (Figure 3D). These data are consistent with previous work in human cells (Pereg et al., 2010) and indicate that Dub3 function in regulating Cdc25A protein stability is analogous in mouse ES cells. In addition, we also observed a role of Dub3 in Cdc25A stability in unperturbed and damaged NIH-3t3 cells (Figure S4C-D). Of note, GFP-tagged Dub3 shows an exclusive nuclear localization (Figure 3E) as previously observed for Cdc25A in ES cells (Koledova et al., 2010). Finally, to address the role of Cdh1 and β-TrCP in regulating Cdc25A levels in ES cells, we performed RNAi-mediated knockdown experiments. In contrast to Dub3 knockdown neither Cdh1, nor β-TrCP downregulation affected Cdc25A mRNA expression nor did significantly alter Cdc25A stability (Figure S4E-F). These observations are consistent with a previous study showing that APC/Cdh1 activity is attenuated in ES cells by high levels of the Emi1 inhibitor (Ballabeni et al., 2011).

Orphan receptor Esrrb regulates Dub3 gene expression

Based on previously described consensus sequence for binding motifs of key transcription factors involved in reprogramming (Chen et al., 2008; Thomson et al., 2011), we analyzed the proximal promoter (6 kb) of the Dub3 gene. Strikingly, while no Oct4, Nanog, Klf4, Smad1, Stat3, c-Myc nor n-Myc consensus sites could be detected, we originally (NCBI37/mm9) found up to seven estrogen-related-receptor-b (Esrrb) putative binding motifs (consensus: 5'-TNAAGGTCA-3')(Deblois et al., 2009) and two Sox2 putative response elements (consensus: 5'-CATTGTT-3'). However the latest update of this genomic sequence (GRCm38/mm10) displays only three Esrrb sites (Figure 4A, Esrrb-RE). Esrrb is a nuclear receptor belonging to the superfamily of nuclear hormone receptors. Together with Sox2, it is part of the core self-renewal machinery (Festuccia et al., 2012; Ivanova et al., 2006; Martello et al., 2012). Esrrb knockdown using a previously validated RNAi sequence (Feng et al., 2009) resulted in significant decrease of endogenous Dub3 transcript level (Figure 4B), to a similar extent than the previously described Esrrb target gene Nanog (van den Berg et al., 2008). Inversely, ectopic expression of Esrrb in ES cells, and not of its C-terminal truncated form (∆-Cter) lacking the activation function 2 (AF2) domain, led to significant increase in endogenous Dub3 mRNA level (Figure 4C). Moreover, treatment of ES cells with increasing dose of DY131, a previously described selective Esrrb and Esrrg agonist (Yu and Forman, 2005), boosted Dub3 gene expression and increased Cdc25A protein abundance without affecting Cdc25A transcript level (Figure S5A-B). Inversely, Esrrb knockdown resulted in a 40% decrease of DY131-mediated Dub3 transcription (Figure S5C), while Sox2 knockdown using a previously published RNAi sequence (Walker et al., 2007) did not strongly affected Dub3 expression, though slightly increased it (our unpublished observations).

Next we performed chromatin immunoprecipitation (ChIP) experiments to map Esrrb and Sox2 binding to Dub3 promoter in ES cells. To this end, we designed five primer pairs (Figure 4A, pp) separated by approximately 1kb to scan promoter occupancy by Esrrb and Sox2 within the 6kb upstream of the start codon (ATG+1). Sonication of chromatin resulted in fragments under 500 bp, limiting signal overlap between primers (Figure S5D). ChIP analysis with an anti-Esrrb antibody (Figure S5E) shows that Esrrb binds to the proximal Dub3 promoter in regions containing the three Esrrb consensus binding motifs (Figure 4D, pp 3-5), while no Esrrb binding was observed in an upstream region that does not contain Esrrb binding sites (pp 1-2). On the contrary, ChIP analysis with an anti-Sox2 antibody showed high enrichment only at one of the two consensus sites in the Dub3 promoter (Sox2-RE2), around primer pair 3, while in the region containing the second site (Sox2-RE1, pp4-5) Sox2 was bound to much lower levels.

To corroborate abovementioned ChIP data, we cloned the Dub3 proximal promoter (3,2 kb) and analyzed its transcriptional activity in a reporter assay using luciferase activity as readout. For this purpose we used cells that have very low expression of endogenous steroid receptors (CV1 cells). As anticipated, we observed strong induction of luciferase activity upon Esrrb expression in cells cotransfected with the 3.2 kb Dub3 promoter that contains all three Esrrb binding sites (Figure 4E, Esrrb, white bars) while only background activity was observed on a region of the Dub3 promoter (5' far) devoid of Esrrb consensus binding sites (Esrrb, black bars). Similarly, expression of Esrrb ∆-Cter, resulted in basal promoter activity, comparable to that observed by expression of empty vector (EV, Figure 4E and S5F). Interestingly, we did not observe stimulation of luciferase activity upon expression of Sox2, but a small and significant repression of basal promoter activity (Figure 4E).

Importantly, mutation of the unique Esrrb binding site in a 1kb Dub3 genomic fragment decreased transcriptional activity (Figure 4F). Altogether these observations suggest that Dub3 is a direct Esrrb target gene, having a positive role in regulating transcription of the Dub3 gene, while Sox2 on its own is not sufficient to stimulate Dub3 transcription.

Developmental regulation of Dub3 expression and Cdc25A stability

Esrrb is a pluripotency factor highly expressed in ES cells that, unlike Sox2, is strongly downregulated upon ES differentiation (Percharde et al., 2012). Since Dub3 is an Esrrb target, we analyzed expression of Dub3 during neural conversion of ES cells *in vitro*. Plating of ES cells in N2B27 culture medium triggers conversion into neuroepithelial precursors (Ying et al., 2003) microscopically visible as rosette conformations (Figure 5A, day 7). Loss of pluripotency was monitored by expression analysis of specific markers such as Oct4, Nanog, Klf4, and acquisition of neural identity was monitored by Nestin and Sox1 expression. Specificity was controlled by analysis of Sox7 expression, a well-established endoderm marker (Figure S6A-B). Importantly, Nestin was detectable in just about each individual cell of the differentiating population at day 6, indicating homogenous neural conversion. Acute (within 24 hours) decrease of Esrrb mRNA expression preceded in time a marked and dramatic decrease of Dub3 expression (Figure 5B). Expression of Sox2 also decreased after 24 hours, however of only 50% and increased afterwards. In contrast, neither Cdc25A nor Cdh1 or β-TrCP transcript levels significantly changed during differentiation (Figure 5B, middle panel). Expression analysis of three other deubiquitylases implicated in Cdc25A stability, USP13, 29 and 48 (Pereg et al., 2010) revealed a decrease of only USP48 within 24 hours after differentiation (Figure 5B,

lower panel) that mirrored Sox2 expression. Importantly, we could not find any consensus Esrrb binding sites within the USP48 proximal promoter. In contrast, USP13 gene expression did not significantly change during differentiation, while USP29 expression strongly increased during neural conversion.

To analyze Dub3 protein levels we raised a specific antibody recognizing, as expected, a 60 kDa polypeptide in SDS-PAGE (Figure S6C-D). Dub3 protein levels dropped massively very early during differentiation, much earlier than Oct4, finely correlating with Dub3 mRNA levels (Figure 5C). Strikingly, lineage commitment between days 2-3, as monitored by Sox1 expression, led to a marked and continuous decrease of Cdc25A protein level, while the protein level of the two other Cdc25 family members, Cdc25B and Cdc25C, remained constant during differentiation (Figure S6E). We further analyzed expression of two additional Dub3 substrates during differentiation, RhoA (de la Vega et al., 2011) and Suds3 (Ramakrishna et al., 2011), and observed no significant variations in gene expression (Figure S6F), nor in protein stability (Figure 5C), although a small decrease in Suds3 level was seen at day 7 after differentiation. Finally, we found very low expression of Esrrg (another member of the subfamily) in ES cells that further increased during differentiation (Figure S6F), corroborating the specificity of Dub3 gene regulation by Esrrb. Altogether, these findings suggest that reduced Cdc25A protein abundance during neural differentiation is likely governed at the post-translational level.

While retaining self-renewal properties, neural stem cells (NSC) are multipotent stem cells derived from ES cells, isolated and amplified at day 7 following differentiation. Quantification of Cdc25A abundance revealed 8-fold more Cdc25A in asynchronously growing ES cells compared to NSCs (Figure 5D). Similar to NIH-3t3 cells, we detected very low Dub3 transcript levels in NSCs (Figure S6G). Finally, we

isolated and analyzed three different genomic fragments of the Dub3 promoter and compared basal transcriptional activity in NIH-3t3 versus ES cells. We observed strong transcriptional activity of all three promoter sequences in ES cells, about 10-fold higher than in NIH-3t3 cells (Figure 5E), further corroborating mRNA expression during differentiation (Figure 5B).

Dub3 expression is important for maintenance of pluripotency and cell cycle remodelling during differentiation

Stable transfection of Esrrb in ES cells has been shown to be sufficient to sustain pluripotency in absence of LIF (Zhang et al., 2008). We therefore addressed whether forced Dub3 expression in ES cells could substitute Essrb function in maintaining pluripotency in absence of LIF. To this end, we generated a stable ES cell line, expanded from a single ES colony, expressing eGFP-Dub3 under control of a constitutive strong promoter (Figure 6A). Remarkably, while Pereg *et al.* (2012) reported that high Dub3 expression induces S-G2/M arrest in human somatic U2OS cells, ES cells overexpressing Dub3 could be propagated without significant differences in cell cycle distribution compared to a control cell line, indicating that in ES cells constitutive Dub3 expression is not toxic (Figure S7A-B). Removal of LIF led to an apparent highly similar morphological differentiation program in both cell-lines, but unexpectedly resulted in massive death of eGFP-Dub3-expressing ES cells two days after, microscopically visible as detached cells with retracted nuclei (Figure 6B, arrows). Of note, five days following LIF withdrawal, hardly any cell survived in the eGFP-Dub3 expressing cell-line. Caspase-3 activity, essential for proper differentiation (Fujita et al., 2008), was higher at days 3-4 in eGFP-Dub3 expressing cells compared to empty vector, strongly indicative of apoptosis (Figure 6C and

Figure S7C). Finally, whereas mRNA and protein levels of pluripotency and differentiation markers were highly comparable in both cell lines, we observed elevated expression of the apoptotic marker Noxa at day two and afterwards in eGFP-Dub3 expressing cells (Figure S7D).

Remarkably, 2-3 days upon LIF removal, a strong reduction of eGFP-Dub3 protein level was evident (Figure 6C), suggesting an additional control at post-transcriptional level, very likely proteolysis, occurring during differentiation. A similar phenotype was observed upon N2B27-mediated neural conversion, and a similar result was also observed with a ES cell line expressing HA N-terminal-tagged Dub3 (Figure S7E-F), ruling out a non-specific effect of the GFP tag or of the differentiation protocol used. Onset of apoptosis, was equally observed by FACS analysis (Figure 6D), that showed the presence of subdiploid (less than 2N) cell debris starting from day three during differentiation and being predominant at day four. Interestingly, appearance of the sub-G1 cell population in ES cells expressing eGFP-Dub3 was concomitant to cell lineage commitment, as monitored by Sox1 and Nestin expression (Figure S6A) and cell cycle remodelling which started at day three in the control cell line (empty vector), resulting in lengthening of the G1 phase (Figure 6D). Altogether these results strongly suggest that high Dub3 expression is lethal during differentiation at the time when cell cycle remodelling occurs.

Finally we analyzed the effect of Dub3 or Cdc25A knockdown in ES cells. Interestingly, prolonged (7 days) RNAi mediated Dub3 knockdown, resulted in an increase of alkaline phosphatase (AP)-negative colonies, as well as heterogeneous morphological differentiation of ES cells even in the presence of LIF, suggesting that Dub3 expression is important for maintenance of pluripotency (Fig 6E-F). A very similar result was also observed upon prolonged Cdc25A knockdown. In sum, these

data couple the self-renewal machinery of ES cells through Essrb to the master cell cycle regulator Cdc25A and remodelling of the cell cycle during differentiation through modulation of Dub3 expression.

Discussion

In this study we dissected the G1/S checkpoint signalling pathway in ES cells. We found that ES cells maintain high levels of the Cdc25A phosphatase in G1 that persists even after DNA damage. Knockdown of Cdc25A expression resulted in a G1 delay and increased CDK2^{Y15P} after UV damage within 24 hours post RNAi treatment (a condition required to avoid natural G1 phase expansion due to differentiation of ES cells). Indeed, prolonged Cdc25A downregulation (or Dub3), resulted in cell differentiation in the presence of LIF, in line with the notion that lengthening of the G1 phase and deregulation of CDK2 activity is linked to differentiation (White et al., 2005). These findings provide an explanation for absent regulation of CDK2 activity upon DNA damage in ES cells (Koledova et al., 2010). This model is also in line with existing evidence linking elevated Cdc25A expression with impaired G1/S arrest followed by radioresistant DNA synthesis in cancer cells (Falck et al., 2001).

Interestingly, in addition to Cdc25A, we have also observed down-regulation of Cyclin E (Figure S6H), another CDK2 regulator that is rate limiting during the G1/S transition and opposes spontaneous differentiation of naïve ES cells (Coronado et al., 2012). Moreover, ablation of the SCF^{Fbw7}-mediated degradation pathway controlling Cyclin E abundance *in vivo* results in impaired differentiation, genomic instability and hyperproliferation (Minella et al., 2008), illustrating the importance of Cyclin E regulation in mouse development. Taken together, both reduced abundance of Cdc25A and Cyclin E during differentiation of ES cells, likely embody key molecular adaptations that control CDK activity and consequent G1 lengthening. Importantly, as a result of expanded G1, the p53-dependent response may now become more effective in CDK2 inhibition since this requires a slow transcriptional-dependent induction of the CDK inhibitor p21 protein level. It is anticipated that p21

may have virtually no role in CDK2 regulation in ES cells since these cells spend most of their time in S phase and p21 is efficiently degraded by the PCNA-dependent $CRL4^{Cdt2}$ ubiquitin ligase throughout S phase, as well as after DNA damage (Abbas et al., 2008).

We have provided evidence that post-transcriptional regulation of Cdc25A abundance in ES cells depends upon the Dub3 deubiquitylase. Expression of Dub3, and not Cdh1 or β-TrCP, is higher in ES cells compared to differentiated cells, and knockdown of Cdh1 or β-TrCP did not significantly change the stability of Cdc25A since it is already highly stabilized in ES cells. These observations are consistent with the finding that ES cells have attenuated APC activity that increases during differentiation (Ballabeni et al., 2011). Of the four additional deubiquitylases implicated in Cdc25A stability in human cells (USP13, 29, 48 and Dub2A), we found that only USP48 mRNA levels significantly decreased during differentiation although its expression remained high and increased towards the end of differentiation, mirroring Sox2 expression. Hence, although we cannot exclude a redundant role for Dub2A and USP48 in Cdc25A stability during differentiation, our data support a key role for Dub3 in this process, as previously shown in somatic cells (Pereg et al., 2010), and suggest that in ES cells the balance of ubiquitylation and deubiquitylation activities, which fine-tunes the steady-state level of Cdc25A, is shifted towards deubiquitylation due to high Dub3 expression.

We showed that downregulation of Esrrb negatively affected the endogenous expression of the Dub3 gene, to a similar extent than a previously characterized Esrrb target gene, Nanog (van den Berg et al., 2008). However, expression of Oct4, another Esrrb target (Zhang et al., 2008) was not found to be much affected by Esrrb knockdown (van den Berg et al., 2008). These differences likely exist because in ES

cells, expression of pluripotency genes is under the combinatorial control of transcription factors of the pluripotency gene regulatory network (van den Berg et al., 2008). This transcriptional control appears to be very complex, gene-specific and remains to be further clarified.

We observed that while forced Dub3 expression could not inhibit differentiation upon LIF withdrawal, unexpectedly it induced massive apoptosis during differentiation concomitant to lineage commitment and cell cycle remodelling, such as lengthening of the G1 phase. These observations are in line with the recent finding that expression of non-degradable Cdc25A mutants leads to early embryonic lethality in mice (E3.5) showing the importance of fine-tuning the expression level of Cdc25A already at the oocyte and morula stages (Bahassi el et al., 2011). Although we have shown that Cdc25A is a critical Dub3 substrate in ES cells, we cannot exclude the implication of other Dub3 substrates (de la Vega et al., 2011; Ramakrishna et al., 2011) in the toxicity observed by forced Dub3 expression during differentiation. The importance of tight Cdc25A regulation during embryogenesis is also underscored by its function in regulation of pluripotency versus differentiation of ES cells since Cdc25A is expressed in progenitor cells undergoing proliferative self-renewing divisions (Peco et al., 2012). We speculate that this developmental regulation might be governed by Dub3 to modify cell cycle dynamics under control of Esrrb.

In conclusion our results couple the Cdc25A-CDK2 cell cycle signalling pathway to the self-renewal machinery through Esrrb-dependent regulation of Dub3 in ES cells, and highlight the importance of deubiquitylases in stem cell and developmental biology. Since cell cycle regulation is a rate-limiting step in reprogramming processes, these findings put Dub3 and Cdc25A as interesting candidate genes in cell reprogramming.

Experimental Procedures

Cell extracts, western blotting and antibodies

Cells were rinsed once in PBS and incubated in lysis buffer. Whole cell extracts were clarified by centrifugation at 12000 *g* for 10 min at 4°C. Protein concentration of was estimated by BCA (Pierce; see Supplemental information).

Cell culture and transfection

ES cells (CGR8) were cultured on gelatin-coated dishes in the absence of feeder cells with 1,000 U LIF per ml (Millipore). Cells were grown in a humidified atmosphere of 5% CO_2 at 37°C. For transient expression both NIH-3t3 and ES cells were transfected using X-tremeGENE 9 DNA (Roche), and CV1 with JetPEI (Polyplus), according to manufacturer's directions. For infection, retroviral particles were generated by transfecting Platinum-E ecotropic packaging cell line with retroviral expression vector (pLPC) encoding Myc_6-Dub3 variants using home-made PEI reagent.

Cell synchronization

ES cells were arrested in prometaphase by nocodazole (Sigma) for 4-8 hours. After mitotic-shake off cells were washed 3 times in ice-cold PBS and dissolved in full ES growth medium. Cells were incubated in a humidified atmosphere of 5% CO_2 at 37°C for 45 minutes and placed at 30°C for 1 hour to reduce S phase entry. Cells were mock- or UV-irradiated (6 J/m^2) and incubated at 37°C prior collection. To synchronise NIH-3t3 cells in G_0 cells were grown to confluence and incubated for 2-3 days. Next, cells were washed, resuspended and split at 30% confluency. Six hours after release, cells were UV-irradiated.

UV-induced DNA Damage and Drugs

UV-C irradiation at 254nm was performed with microprocessor-controlled crosslinker (BIO-LINK ®) or with a UV-lamp (Hanovia). Cycloheximide and DY131 (GW4716) were from Sigma and Chk1 inhibitor SB218078 from Calbochiem.

Flow cytometry

Single-cell suspensions were prepared by trypsinisation and washed once in PBS. Cells were fixed in ice-cold 70% ethanol (-20°C) and stored at -20 °C overnight. Following RNAse A treatment, total DNA was stained with propidium iodide (25 µg/ml). For BrdU uptake analysis, ES cells and NIH-3t3 cells were grown in the presence of 10 µM BrdU for respectively 10 and 30 minutes. The BrdU content was determined by reaction with a fluorescein isothiocyanate (FITC)-conjugated anti-BrdU antibody (BD Biosciences). Cells were analyzed with a FACScalibur flow cytometer using CellQuestPro software.

RNA extraction, reverse transcription and quantitative real-time PCR

Total RNA was isolated with TRIzol reagent (Invitrogen). Reverse transcription was carried out with random hexanucleotides (Sigma) and Superscript II First-Strand cDNA synthesis kit (Invitrogen). Quantitative PCRs were performed using Lightcycler SYBR Green I Master mix (Roche) on Lightcycler apparatus (Roche). All primers used were intronspanning (primer sequences available upon request). The relative amount of target cDNA was obtained by normalisation using geometric averaging of multiple internal control genes (ACTB, HPRT, HMBS, GAPDH, SDHA).

Chromatin Immunoprecipitation

ES cells were formaldehyde cross-linked and sonicated using a Misonix sonicator S-4000. Cells were lysed in ice-cold lysis buffer (Supplemental Information). Primer pairs for promoter scanning (6 kb upstream of transcription start site, TSS) of the Dub3 murine promoter were designed approximately every 1 kb.

Monolayer differentiation of ES cells into neurectodermal precursors

This protocol was as previously described (Ying et al., 2003). (see also Supplemental information).

Isolation and amplification of NSC cells from CGR8 ES cells

ES cells were induced to differentiate into NSC following the protocol described above. At day 6, cells were dissociated in 0.01% Trypsine-EDTA and plated onto Poly-L-Ornithine/Laminin coated dishes in DMEM/N2 medium with 10 ng/ml of both EGF and bFGF (Biosource). For the preparation of Poly-L-Ornithine/Laminin plates, a 0.01% solution of poly-L-ornithine (Sigma) was added to plates for at least 20 min. The solution was removed and plates were washed 3 times with PBS. A 1 µg/ml solution of laminin in PBS (Sigma) was then applied and incubated at 37°C for at least 3 hrs. Cells can then be cultivated and amplified under these conditions for several subpassages without loosing neural stem cells properties.

Establishment of a monoclonal eGFP-Dub3 expressing ES cells

Wild-type ES cells were transfected with pcDNA3-eGFPDub3, plated at clonal density and selected with G418 (Sigma). eGFP-Dub3 positive clones were expanded

in continuous presence of G418 and validated by immunofluorescence and western blotting.

Acknowledgments

We thank J-M. Vanacker for Esrrb vectors, H. Te Riele for $p53^{-/-}$ ES cells, P. Stambrook and S. Manenti for Cdc25A wild-type and mutant cDNAs, J. Basbous for p53 reporter constructs, and F. Poulat for Sox2 vector. We also thank P. Coulombe and F. Cammas for technical assistance, and D. Hodroj, E. Golfetto and I. Peiffer for technical support. We tank V. Dulic and D. Fisher for critical reading of the manuscript. This project was supported from grants from ARC (grant N° 3156 to D.M. and personal fellowship to S. v. d. L) and FRM (“Equipes”).

Figure Legends

Figure 1: DNA damage in G1 induces transient ES cell cycle arrest in early S-phase and not at the G1/S transition.

(A) Schematic overview of the experimental design. Arrows indicate time points at which cells were collected.

(B) FACS analysis of ES cells released from nocodazole arrest, mock (left panel) or exposed to 6 J/m^2 UV light (right panel) in G1. Analysis of total DNA content stained by propidium iodide at indicated time points.

(C-D) Kinetics of S phase entry of synchronised ES cells, mock and UV-irradiated (6 J/m^2) in G1. Cell cycle distribution was measured by BrdU incorporation followed by FACS analysis.

(E) Representative FACS analysis of S-phase entry by analysis of BrdU immunoreactivity of ES and NIH-3t3 cells exposed respectively to 6 and 10 J/m^2 UV light in G1. Box indicates region were differences in total events was observed. Mean fluorescence intensity of BrdU-positive cells is shown. (see also Figure S1).

Figure 2: Persistence of Cdc25A upon DNA damage in G1 sustains G1/S checkpoint bypass in ES cells.

(A) Asynchronously growing ES and NIH-3t3 cells were exposed to 10 J/m^2 of UV-light, collected and analyzed by western blotting at the indicated times. For Cdc25A, a dark and light exposure is shown.

(B) Abundance of Cdc25A in ES and NIH-3t3 cells synchronized in G1 and passing through S phase. ES cells were synchronized by nocodazole and collected upon release at indicated time points. NIH-3t3 cells were synchronized by confluence, released and collected at 6 hours (G1) and 18 hours (S) after release. To observe

posttranslational modifications (PTM) of Cdc25A, dark and light western blot exposure is shown.

(C) Western blot analysis of Flag-immunoprecipitated, ectopically expressed Flag-Cdc25A cotransfected with HA-ubiquitin in ES (lane 1) and NIH-3t3 cells (lane 2) after MG132 treatment for 1 hour. IgGs indicates immunoglobulins.

(D) Rapid Cdc25A destruction upon DNA damage is Chk1-dependent in ES cells. Cells were UV-irradiated and incubated with cycloheximide (Cx) in absence or presence of Chk1 inhibitor SB218078, collected at the indicated times (min) and analyzed by western blotting.

(E) Downregulation of Cdc25A expression by RNAi results in increased inhibitory $CDK2^{Tyr15}$ phosphorylation upon DNA damage in G1. RNAi-transfected cells were released from nocodazole and exposed to UV-light in G1. Samples were collected at the indicated times and analyzed by western blotting with the indicated antibodies.

(F) Cdc25A downregulation results in G1 delay upon DNA damage. RNAi-transfected cells were released from nocodazole and exposed to UV light in G1 (t=2) and collected 2 hours (t=4) after UV- or mock-irradiation. Prior to collection cells were pulse-labelled with BrdU. Fraction (expressed as %) of diploid BrdU negative cells is plotted (data are represented as mean $\pm$ SD). Statistical differences is indicated with a single asterisk (*) for $P < 0.05$. (see also Figure S3).

Figure 3: Elevated deubiquitylase Dub3 in ES cells increases Cdc25A abundance.

(A) qPCR quantification of Oct4, Cdc25A, Cdh1, β-TrCP and Dub3 mRNA normalized to multiple reference genes in ES and NIH-3t3 cells. Data are expressed as mean $\pm$ SD (error bars) of multiple observations. Statistical differences is indicated with an asterisk $P < 0.05$.

(B) qPCR quantification of Dub3 mRNA normalised to multiple reference genes. ES cells were transfected with control (Crtl), Dub3 or Cdc25A RNAi sequences.

(C) qPCR quantification of Cdc25A mRNA normalised to multiple reference genes. ES cells were transfected with control (Crtl), Dub3 or Cdc25A RNAi sequences.

(D) Western blot analysis of ES cells transfected with Dub3, Cdc25A or control (Crtl) RNAi sequences.

(E) Cellular localisation of pcDNA3-eGFP-Dub3 in ES cells. Nuclei were counterstained using DAPI. Scale bar 10 µM. (See also Figure S4).

Figure 4: Dub3 is a target gene of the orphan receptor Esrrb.

(A) Schematic overview of the Dub3 proximal promoter in mouse (6kb). Esrrb (shaded boxes) and Sox2 (green boxes) consensus binding sites (RE) are indicated.

(B) qPCR quantification of Esrrb, Dub3 and Nanog mRNA normalised to multiple reference genes expressed as % of control. ES cells were transfected with control (Crtl) RNAi (white bars) or Esrrb specific RNAi sequence (black bars). Data are expressed as mean ± SD (error bars) of multiple observations. Statistical differences is indicated with a single asterisk (*) for $P < 0.05$, not significant is indicated as (ns).

(C) qPCR quantification of endogenous Dub3 expression in ES cells transfected with empty vector (EV), Esrrb or Esrrb-ΔCter expressing plasmids. Data are expressed as mean ± SD (error bars) of multiple observations. Statistical differences is indicated with a single asterisk (*) for $P < 0.05$.

(D) ChIP of Esrrb and Sox2 on Dub3 promoter. Primer pair location along the 6 kb proximal promoter (Figure 4A) for scanning of Dub3 promoter for Esrrb and Sox2 occupancy. Data are expressed as mean ± SD (error bars) of multiple observations.

Amylase serves here as a control. Statistical analysis using two-way ANOVA was performed.

(E) Dub3 promoter activity using luciferase assay in CV1 cells. Cells were cotransfected with promoter construct and the indicated genes, and assessed for luciferase activity 48 hours post-transfection. Bars represent the fold induction ± SD of multiple observations. Statistical differences is indicated with a single asterisk (*) for $P < 0.05$ and (**) for $P < 0.001$.

(F) Basal transcriptional activity of a 1 kb proximal promoter and a mutated sequence in ES cells. Three mutations were introduced in the Esrrb consensus binding site. TCAAGGTCA was mutated to TCATTTTCA. Data are expressed as mean ± SD (error bars) of multiple observations (see also Figure S5).

Figure 5: Developmental regulation of Cdc25A protein abundance correlates with Dub3 expression.

(A) N2B27-induced neural conversion of ES cells. Phase-contrast photos at indicated days of differentiation.

(B) qPCR quantification of indicated mRNA normalised to multiple reference genes during N2B27-induced neural differentiation. Values represent mean ± SD of multiple observations.

(C) Western blot analysis of cell extracts collected throughout differentiation of ES cells into neural stem cells (NSC) immunoblotted with the indicated antibodies.

(D) Western blot analysis of asynchronously growing ES and NSC. Cells were exposed to 6 J/m^2 UV-light and collected at indicated times.

(E) Basal transcriptional activity of three different promoter lengths of the Dub3 gene analysed in NIH-3t3 cells and ES cells. Data are expressed as mean ± SD (error bars) of multiple observations (see also Figure S6).

Figure 6: Constitutive Dub3 expression leads to massive apoptosis concomitant to differentiation-induced cell cycle remodeling.

(A) Immunofluorescence detection of empty vector (EV) or eGFP-Dub3-expressing cells. All ES cells express eGFP-Dub3 at comparable levels. DNA was visualized by DAPI staining.

(B) Phase-contrast photos of empty vector (EV) or eGFP-Dub3-expressing ES cells after LIF removal at the indicated days of differentiation. Arrows indicate detached cells with apoptotic morphology.

(C) Western blot of cell extracts prepared every day after LIF withdrawal from empty vector or eGFP-Dub3-expressing ES cells. (*) indicates a non-specific band. High caspase 3 activities in eGFP-Dub3 expressing cells indicate apoptosis.

(D) Differentiation-induced cell cycle remodelling. Cells were collected at the indicated days and analyzed by FACS following propidium iodide staining. Cell death is illustrated by cells with subdiploid DNA content (Sub-G1).

(E) Clonogenic assay of ES cells upon prolonged control or Dub3 targeting RNAi sequence. Cells were plated at clonal density in LIF-containing serum and stained for AP after 7 days. Columns show the percentage of AP positive (Pos.) or negative (Neg.) colonies. At least 150 colonies were scored.

(F) Representative pictures of cells transfected with control or Dub3 targeting RNAi sequence and assayed for AP activity (see also Figure S7).

References

Abbas, T., Sivaprasad, U., Terai, K., Amador, V., Pagano, M., and Dutta, A. (2008). PCNA-dependent regulation of p21 ubiquitylation and degradation via the CRL4Cdt2 ubiquitin ligase complex. Genes Dev *22*, 2496-2506.

Aladjem, M.I., Spike, B.T., Rodewald, L.W., Hope, T.J., Klemm, M., Jaenisch, R., and Wahl, G.M. (1998). ES cells do not activate p53-dependent stress responses and undergo p53-independent apoptosis in response to DNA damage. Curr Biol *8*, 145-155.

Bahassi el, M., Yin, M., Robbins, S.B., Li, Y.Q., Conrady, D.G., Yuan, Z., Kovall, R.A., Herr, A.B., and Stambrook, P.J. (2011). A human cancer-predisposing polymorphism in Cdc25A is embryonic lethal in the mouse and promotes ASK-1 mediated apoptosis. Cell Div *6*, 4.

Ballabeni, A., Park, I.H., Zhao, R., Wang, W., Lerou, P.H., Daley, G.Q., and Kirschner, M.W. (2011). Cell cycle adaptations of embryonic stem cells. Proc Natl Acad Sci U S A *108*, 19252-19257.

Buckley, S.M., Aranda-Orgilles, B., Strikoudis, A., Apostolou, E., Loizou, E., Moran-Crusio, K., Farnsworth, C.L., Koller, A.A., Dasgupta, R., Silva, J.C., *et al.* (2012). Regulation of pluripotency and cellular reprogramming by the ubiquitin-proteasome system. Cell Stem Cell *11*, 783-798.

Busino, L., Chiesa, M., Draetta, G.F., and Donzelli, M. (2004). Cdc25A phosphatase: combinatorial phosphorylation, ubiquitylation and proteolysis. Oncogene *23*, 2050-2056.

Busino, L., Donzelli, M., Chiesa, M., Guardavaccaro, D., Ganoth, D., Dorrello, N.V., Hershko, A., Pagano, M., and Draetta, G.F. (2003). Degradation of Cdc25A by beta-TrCP during S phase and in response to DNA damage. Nature *426*, 87-91.

Chen, T., Du, J., and Lu, G. (2012). Cell growth arrest and apoptosis induced by Oct4 or Nanog knockdown in mouse embryonic stem cells: a possible role of Trp53. Mol Biol Rep *39*, 1855-1861.

Chen, X., Xu, H., Yuan, P., Fang, F., Huss, M., Vega, V.B., Wong, E., Orlov, Y.L., Zhang, W., Jiang, J., *et al.* (2008). Integration of external signaling pathways with the core transcriptional network in embryonic stem cells. Cell *133*, 1106-1117.

Ciccia, A., and Elledge, S.J. (2010). The DNA damage response: making it safe to play with knives. Mol Cell *40*, 179-204.

Coronado, D., Godet, M., Bourillot, P.Y., Tapponnier, Y., Bernat, A., Petit, M., Afanassieff, M., Markossian, S., Malashicheva, A., Iacone, R., *et al.* (2012). A short G1 phase is an intrinsic determinant of naive embryonic stem cell pluripotency. Stem Cell Res *10*, 118-131.

de la Vega, M., Kelvin, A.A., Dunican, D.J., McFarlane, C., Burrows, J.F., Jaworski, J., Stevenson, N.J., Dib, K., Rappoport, J.Z., Scott, C.J., *et al.* (2011). The deubiquitinating enzyme USP17 is essential for GTPase subcellular localization and cell motility. Nat Commun *2*, 259.

Deblois, G., Hall, J.A., Perry, M.C., Laganiere, J., Ghahremani, M., Park, M., Hallett, M., and Giguere, V. (2009). Genome-wide identification of direct target genes implicates estrogen-related receptor alpha as a determinant of breast cancer heterogeneity. Cancer Res *69*, 6149-6157.

Donzelli, M., Squatrito, M., Ganoth, D., Hershko, A., Pagano, M., and Draetta, G.F. (2002). Dual mode of degradation of Cdc25 A phosphatase. EMBO J *21*, 4875-4884.

Falck, J., Mailand, N., Syljuasen, R.G., Bartek, J., and Lukas, J. (2001). The ATM-Chk2-Cdc25A checkpoint pathway guards against radioresistant DNA synthesis. Nature *410*, 842-847.

Feng, B., Jiang, J., Kraus, P., Ng, J.H., Heng, J.C., Chan, Y.S., Yaw, L.P., Zhang, W., Loh, Y.H., Han, J., *et al.* (2009). Reprogramming of fibroblasts into induced pluripotent stem cells with orphan nuclear receptor Esrrb. Nat Cell Biol *11*, 197-203.
Festuccia, N., Osorno, R., Halbritter, F., Karwacki-Neisius, V., Navarro, P., Colby, D., Wong, F., Yates, A., Tomlinson, S.R., and Chambers, I. (2012). Esrrb is a direct Nanog target gene that can substitute for Nanog function in pluripotent cells. Cell Stem Cell *11*, 477-490.
Festuccia, N., Osorno, R., Wilson, V., and Chambers, I. (2013). The role of pluripotency gene regulatory network components in mediating transitions between pluripotent cell states. Current opinion in genetics & development.
Fujita, J., Crane, A.M., Souza, M.K., Dejosez, M., Kyba, M., Flavell, R.A., Thomson, J.A., and Zwaka, T.P. (2008). Caspase activity mediates the differentiation of embryonic stem cells. Cell Stem Cell *2*, 595-601.
Gautier, E.F., Picard, M., Laurent, C., Marty, C., Villeval, J.L., Demur, C., Delhommeau, F., Hexner, E., Giraudier, S., Bonnevialle, N., *et al.* (2012). The cell cycle regulator CDC25A is a target for JAK2V617F oncogene. Blood *119*, 1190-1199.
Hong, Y., and Stambrook, P.J. (2004). Restoration of an absent G1 arrest and protection from apoptosis in embryonic stem cells after ionizing radiation. Proc Natl Acad Sci U S A *101*, 14443-14448.
Ivanova, N., Dobrin, R., Lu, R., Kotenko, I., Levorse, J., DeCoste, C., Schafer, X., Lun, Y., and Lemischka, I.R. (2006). Dissecting self-renewal in stem cells with RNA interference. Nature *442*, 533-538.
Karnani, N., and Dutta, A. (2011). The effect of the intra-S-phase checkpoint on origins of replication in human cells. Genes Dev *25*, 621-633.
Koledova, Z., Kafkova, L.R., Kramer, A., and Divoky, V. (2010). DNA damage-induced degradation of Cdc25A does not lead to inhibition of Cdk2 activity in mouse embryonic stem cells. Stem Cells *28*, 450-461.
Mailand, N., Falck, J., Lukas, C., Syljuasen, R.G., Welcker, M., Bartek, J., and Lukas, J. (2000). Rapid destruction of human Cdc25A in response to DNA damage. Science *288*, 1425-1429.
Malumbres, M., and Barbacid, M. (2001). To cycle or not to cycle: a critical decision in cancer. Nat Rev Cancer *1*, 222-231.
Martello, G., Sugimoto, T., Diamanti, E., Joshi, A., Hannah, R., Ohtsuka, S., Gottgens, B., Niwa, H., and Smith, A. (2012). Esrrb is a pivotal target of the Gsk3/Tcf3 axis regulating embryonic stem cell self-renewal. Cell Stem Cell *11*, 491-504.
Minella, A.C., Loeb, K.R., Knecht, A., Welcker, M., Varnum-Finney, B.J., Bernstein, I.D., Roberts, J.M., and Clurman, B.E. (2008). Cyclin E phosphorylation regulates cell proliferation in hematopoietic and epithelial lineages in vivo. Genes Dev *22*, 1677-1689.
Neganova, I., Vilella, F., Atkinson, S.P., Lloret, M., Passos, J.F., von Zglinicki, T., O'Connor, J.E., Burks, D., Jones, R., Armstrong, L., *et al.* (2011). An important role for CDK2 in G1 to S checkpoint activation and DNA damage response in human embryonic stem cells. Stem Cells *29*, 651-659.
Neganova, I., Zhang, X., Atkinson, S., and Lako, M. (2009). Expression and functional analysis of G1 to S regulatory components reveals an important role for CDK2 in cell cycle regulation in human embryonic stem cells. Oncogene *28*, 20-30.
Peco, E., Escude, T., Agius, E., Sabado, V., Medevielle, F., Ducommun, B., and Pituello, F. (2012). The CDC25B phosphatase shortens the G2 phase of neural progenitors and promotes efficient neuron production. Development *139*, 1095-1104.

Percharde, M., Lavial, F., Ng, J.H., Kumar, V., Tomaz, R.A., Martin, N., Yeo, J.C., Gil, J., Prabhakar, S., Ng, H.H., *et al.* (2012). Ncoa3 functions as an essential Esrrb coactivator to sustain embryonic stem cell self-renewal and reprogramming. Genes & development *26*, 2286-2298.
Pereg, Y., Liu, B.Y., O'Rourke, K.M., Sagolla, M., Dey, A., Komuves, L., French, D.M., and Dixit, V.M. (2010). Ubiquitin hydrolase Dub3 promotes oncogenic transformation by stabilizing Cdc25A. Nat Cell Biol *12*, 400-406.
Prost, S., Bellamy, C.O., Clarke, A.R., Wyllie, A.H., and Harrison, D.J. (1998). p53-independent DNA repair and cell cycle arrest in embryonic stem cells. FEBS Lett *425*, 499-504.
Ramakrishna, S., Suresh, B., Lee, E.J., Lee, H.J., Ahn, W.S., and Baek, K.H. (2011). Lys-63-specific deubiquitination of SDS3 by USP17 regulates HDAC activity. J Biol Chem *286*, 10505-10514.
Sabapathy, K., Klemm, M., Jaenisch, R., and Wagner, E.F. (1997). Regulation of ES cell differentiation by functional and conformational modulation of p53. EMBO J *16*, 6217-6229.
Savatier, P., Lapillonne, H., Jirmanova, L., Vitelli, L., and Samarut, J. (2002). Analysis of the cell cycle in mouse embryonic stem cells. Methods Mol Biol *185*, 27-33.
Sexl, V., Diehl, J.A., Sherr, C.J., Ashmun, R., Beach, D., and Roussel, M.F. (1999). A rate limiting function of cdc25A for S phase entry inversely correlates with tyrosine dephosphorylation of Cdk2. Oncogene *18*, 573-582.
Solozobova, V., Rolletschek, A., and Blattner, C. (2009). Nuclear accumulation and activation of p53 in embryonic stem cells after DNA damage. BMC Cell Biol *10*, 46.
Stead, E., White, J., Faast, R., Conn, S., Goldstone, S., Rathjen, J., Dhingra, U., Rathjen, P., Walker, D., and Dalton, S. (2002). Pluripotent cell division cycles are driven by ectopic Cdk2, cyclin A/E and E2F activities. Oncogene *21*, 8320-8333.
Thomson, M., Liu, S.J., Zou, L.N., Smith, Z., Meissner, A., and Ramanathan, S. (2011). Pluripotency factors in embryonic stem cells regulate differentiation into germ layers. Cell *145*, 875-889.
van den Berg, D.L., Zhang, W., Yates, A., Engelen, E., Takacs, K., Bezstarosti, K., Demmers, J., Chambers, I., and Poot, R.A. (2008). Estrogen-related receptor beta interacts with Oct4 to positively regulate Nanog gene expression. Mol Cell Biol *28*, 5986-5995.
Walker, E., Ohishi, M., Davey, R.E., Zhang, W., Cassar, P.A., Tanaka, T.S., Der, S.D., Morris, Q., Hughes, T.R., Zandstra, P.W., *et al.* (2007). Prediction and testing of novel transcriptional networks regulating embryonic stem cell self-renewal and commitment. Cell Stem Cell *1*, 71-86.
White, J., Stead, E., Faast, R., Conn, S., Cartwright, P., and Dalton, S. (2005). Developmental activation of the Rb-E2F pathway and establishment of cell cycle-regulated cyclin-dependent kinase activity during embryonic stem cell differentiation. Mol Biol Cell *16*, 2018-2027.
Ying, Q.L., Stavridis, M., Griffiths, D., Li, M., and Smith, A. (2003). Conversion of embryonic stem cells into neuroectodermal precursors in adherent monoculture. Nat Biotechnol *21*, 183-186.
Yu, D.D., and Forman, B.M. (2005). Identification of an agonist ligand for estrogen-related receptors ERRbeta/gamma. Bioorg Med Chem Lett *15*, 1311-1313.
Zhang, X., Neganova, I., Przyborski, S., Yang, C., Cooke, M., Atkinson, S.P., Anyfantis, G., Fenyk, S., Keith, W.N., Hoare, S.F., *et al.* (2009). A role for NANOG in G1 to S transition in human embryonic stem cells through direct binding of CDK6 and CDC25A. J Cell Biol *184*, 67-82.

Zhang, X., Zhang, J., Wang, T., Esteban, M.A., and Pei, D. (2008). Esrrb activates Oct4 transcription and sustains self-renewal and pluripotency in embryonic stem cells. J Biol Chem *283*, 35825-35833.

Figure1
Click here to download high resolution image

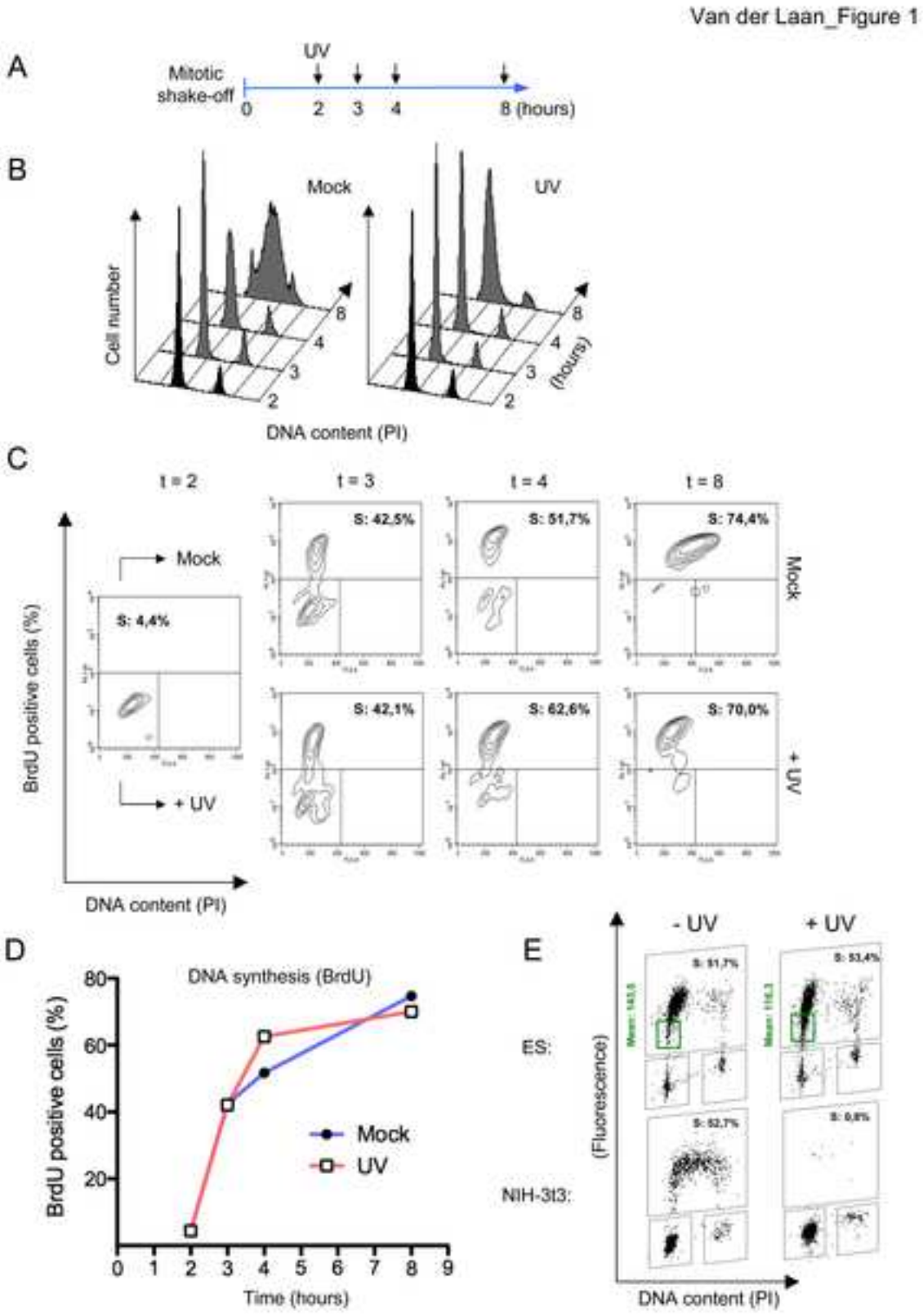

Figure2
Click here to download high resolution image

Van der Laan_Figure 2

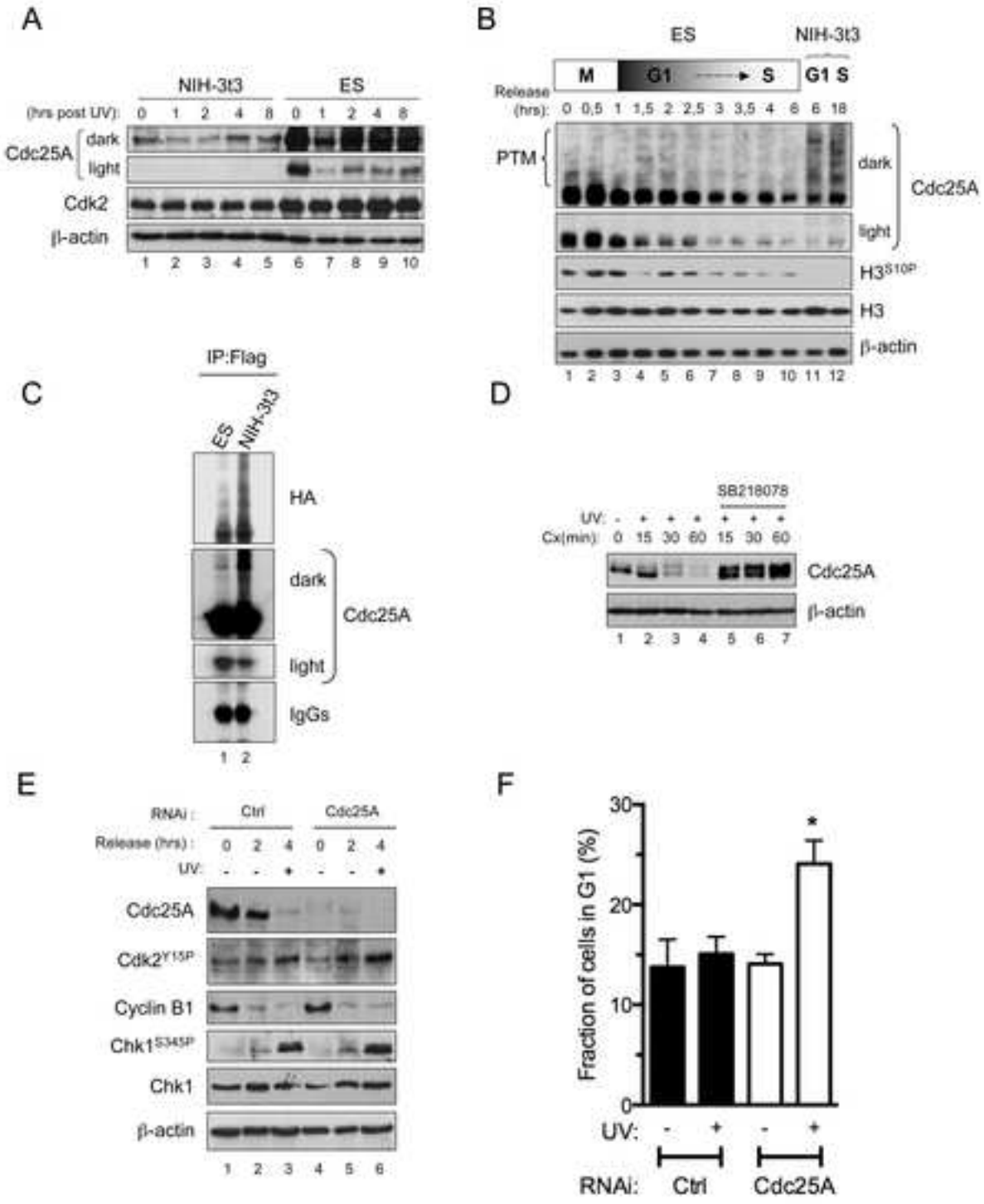

Figure3
Click here to download high resolution image

Van der Laan_Figure 3

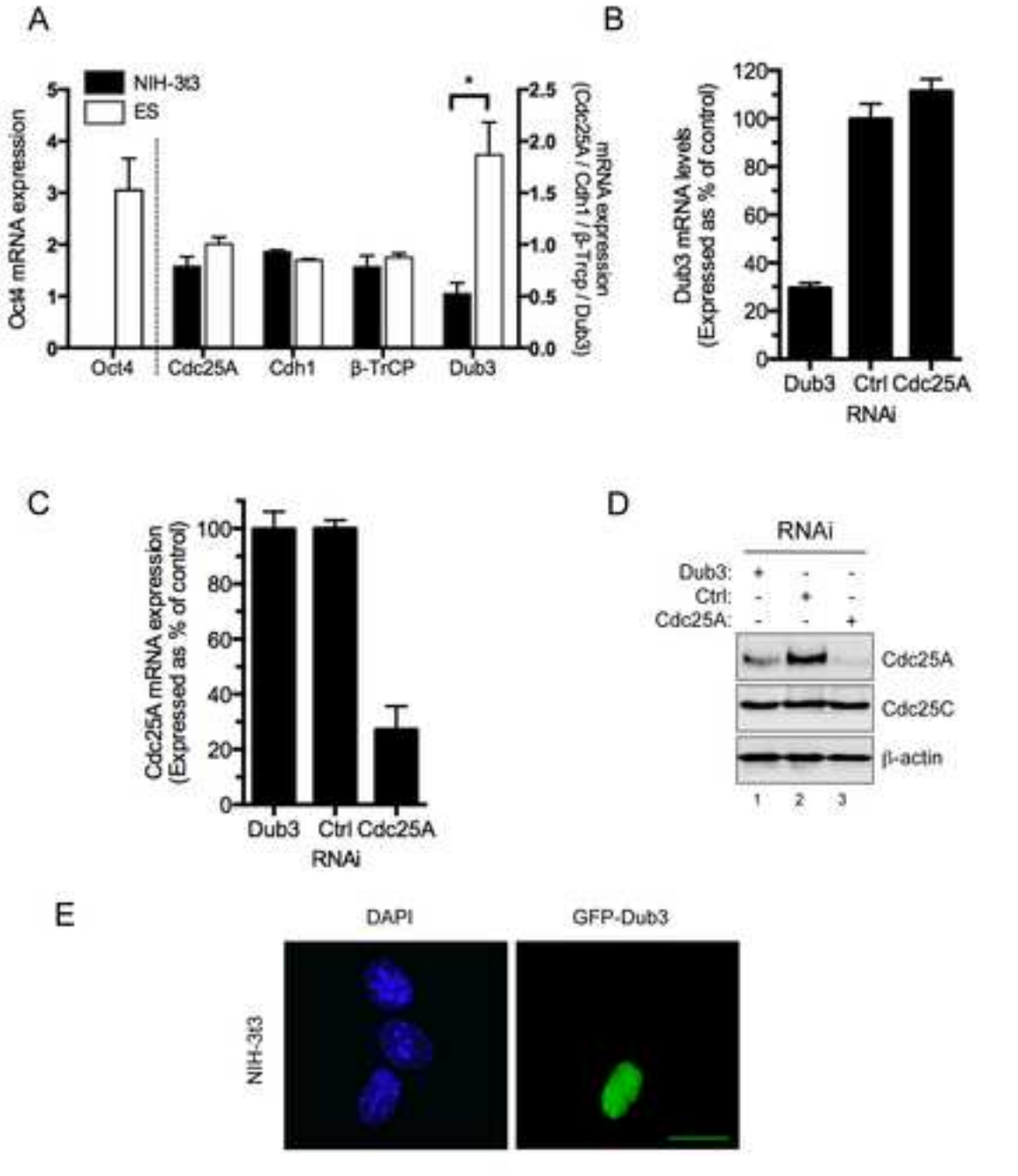

Figure4
Click here to download high resolution image

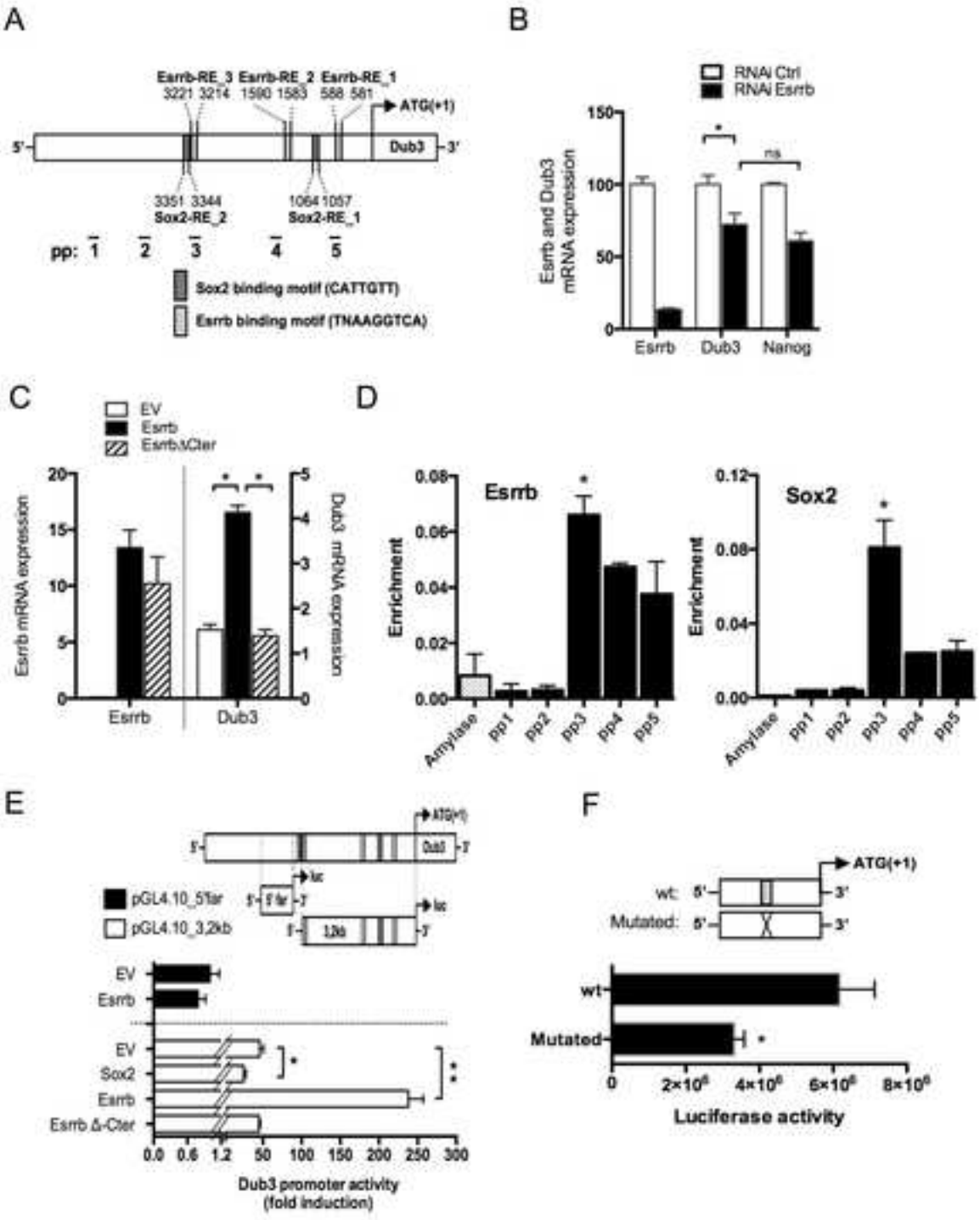

Figure5
Click here to download high resolution image

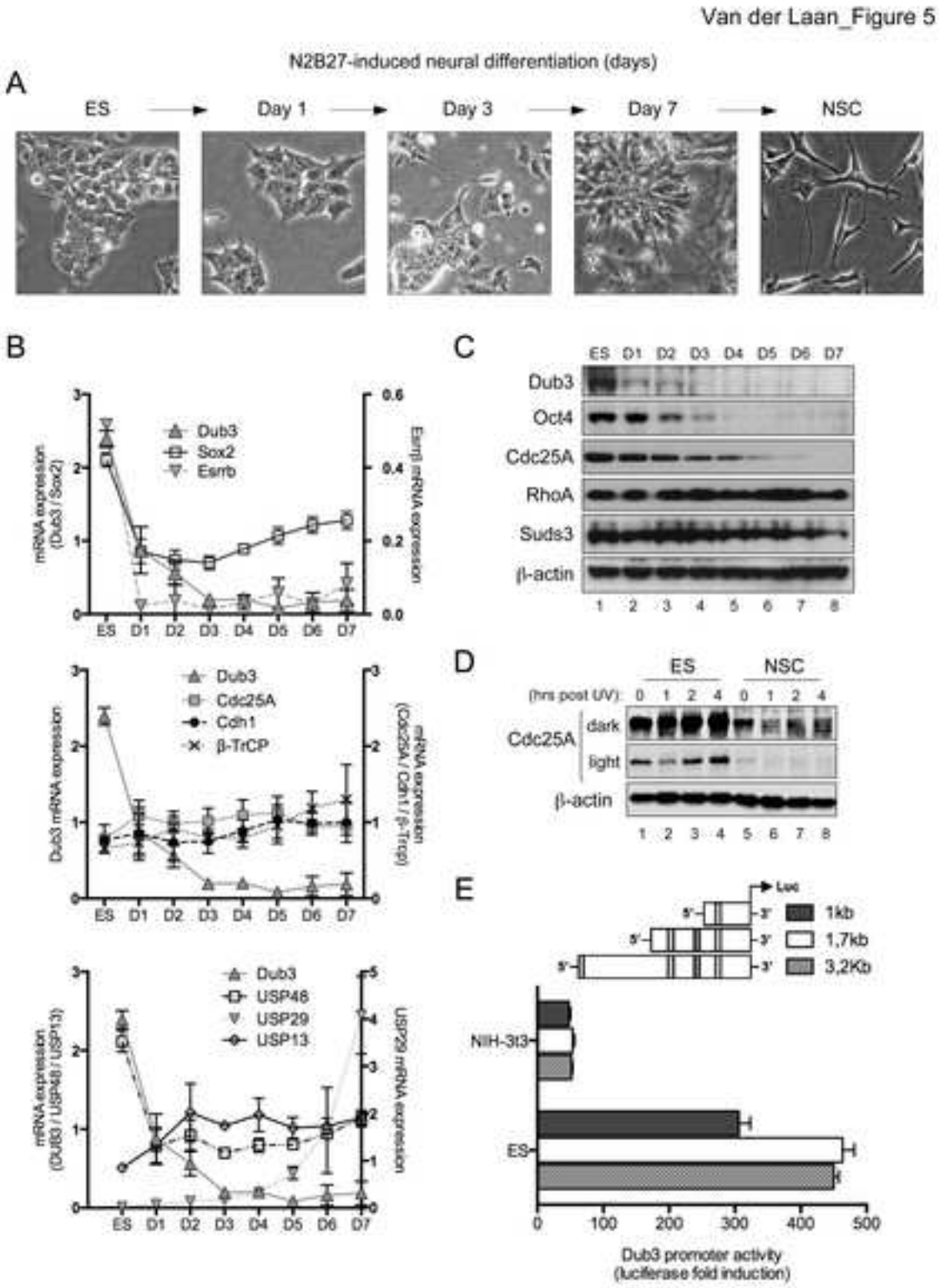

Figure6
Click here to download high resolution image

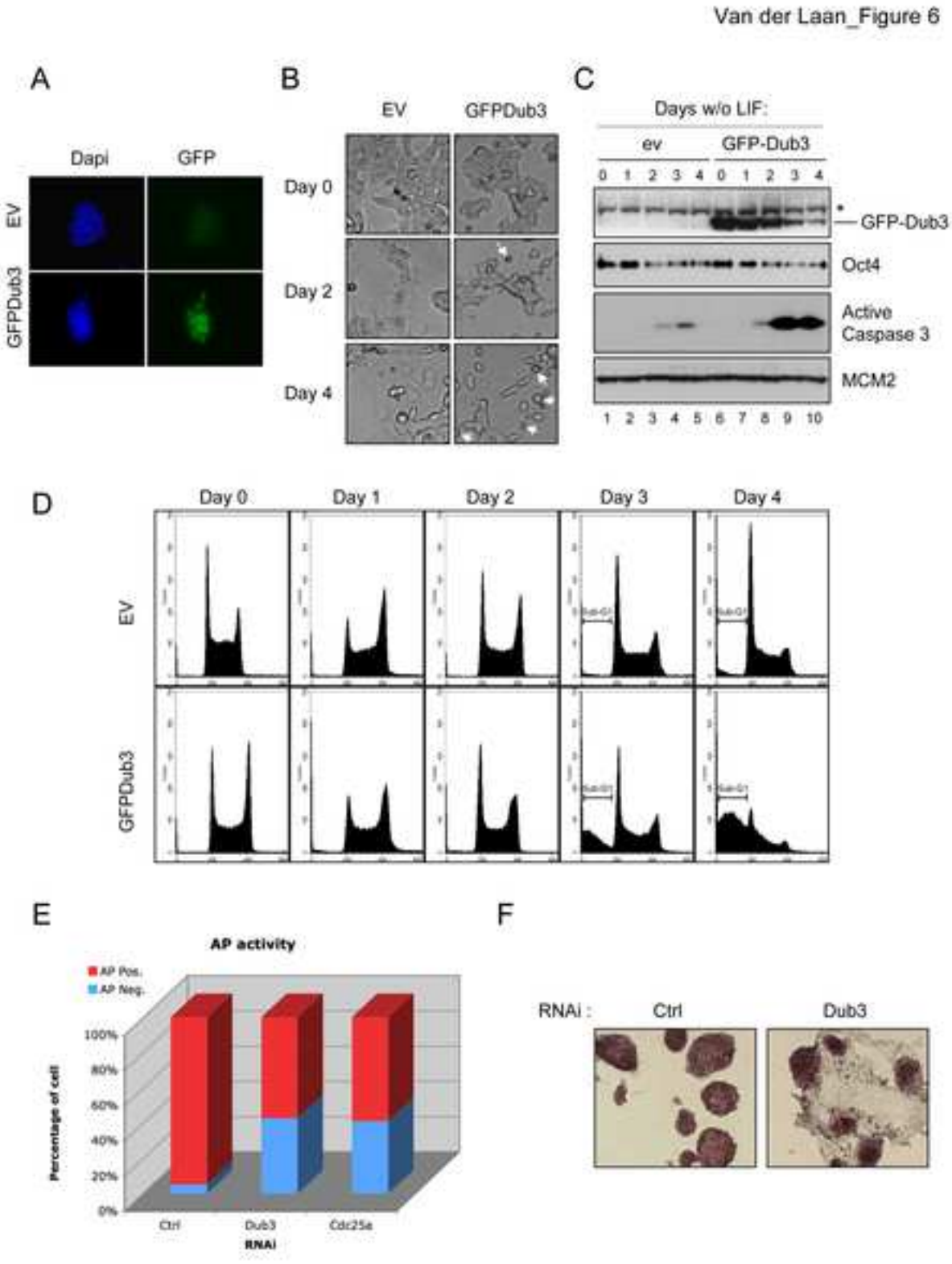

Inventory of Supplemental Information

High Dub3 expression in mouse ES cells couples pluripotency to the G1/S checkpoint

Siem VAN DER LAAN, Nikolay TSANOV, Carole CROZET and Domenico MAIORANO

Supplemental information:

Seven Supplemental Figures, Figures legends and Supplemental experimental procedures.

Figure S1 (related to Figure 1). Shows additional information providing evidence for an arrest of mouse embryonic stem cells in early S phase and not in G1 upon UV damage.

Figure S2 (related to Figure 1). Shows that the p53 transcriptional response is functional in mouse embryonic stem cells upon UV damage.

Figure S3 (related to Figure 2). Provides additional information showing that Cdcd25A is more abundant in mouse embryonic stem cells than in differentiated NIH-3T3 cells and that the G1/S transition in mouse embryonic stem cells requires CDK2 activity. It also shows that fluctuation of Cdc25A levels correlate with changes in CDK2 tyrosine 15 phosphorylation which is increased following Cdc25A downregulation upon UV damage.

Figure S4 (related to Figure 3). Provides evidence that Cdc25A half-life is higher in mouse embryonic stem cells than in differentiated NIH-3T3 cells. Moreover it provides supplementary evidence that Dub3 and not Cdh1 nor b-TRCP regulates Cdc25A stability in mouse embryonic stem cells.

Figure S5 (related to Figure 4). Shows that the Esrrb and Esrrg agonist DY131 boosts Dub3 expression in mouse embryonic stem cells. It also provides important controls for the Chip experiments.

Figure S6 (related to Figure 5). Provides additional data essential to control the differentiation of mouse embryonic stem cells into neural stem cells (NSCs), essential to interpret the results shown in Figure 5. It also shows the specificity of the mouse Dub3 antibody.

Figure S7 (related to Figure 6). Provides additional information for the cell death observed in mouse embryonic stem cells expressing eGFP-Dub3 and undergoing differentiation. It also shows that a similar phenotype is observed in cells expressing HA-Dub3.

Van der Laan_Figure S1

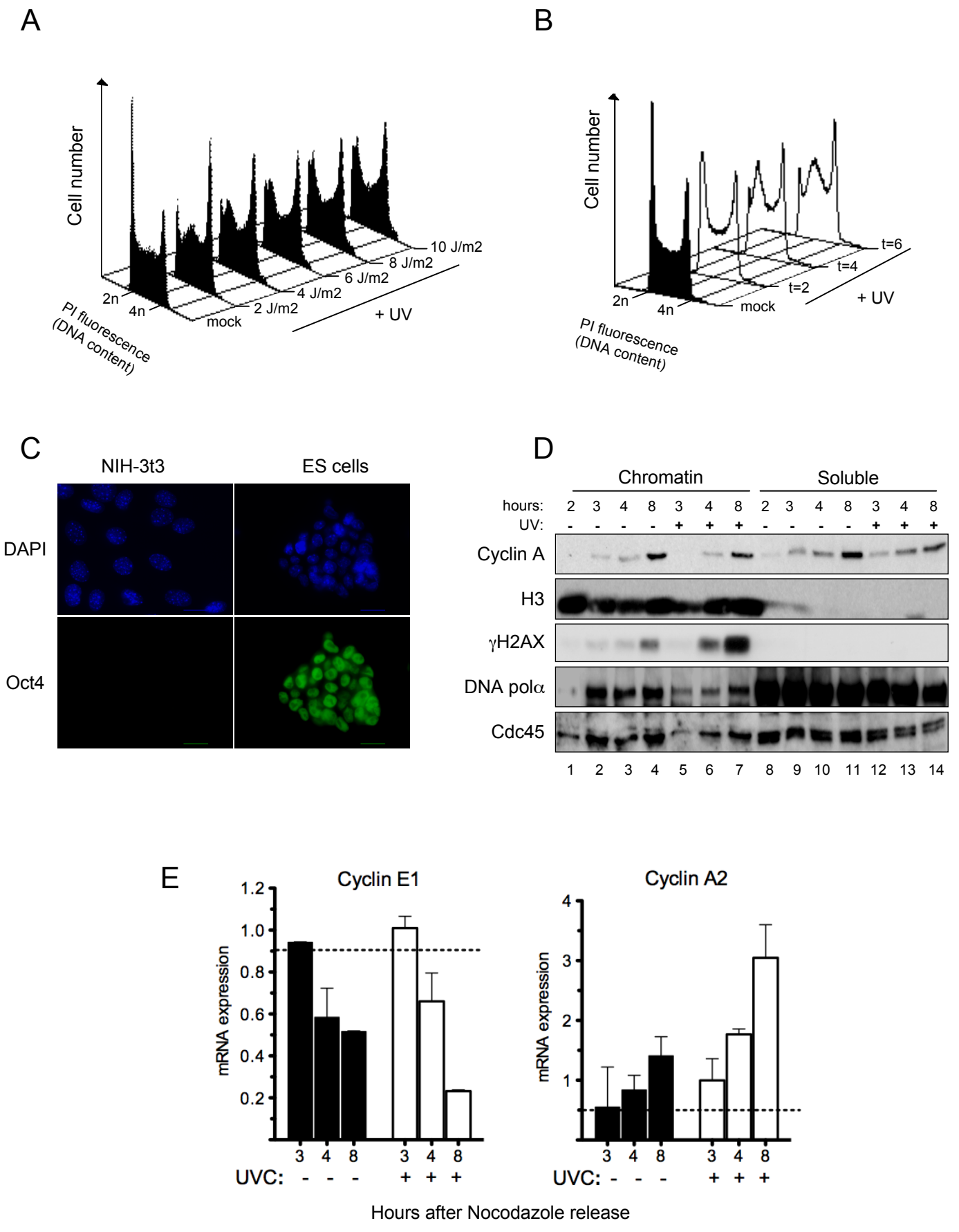

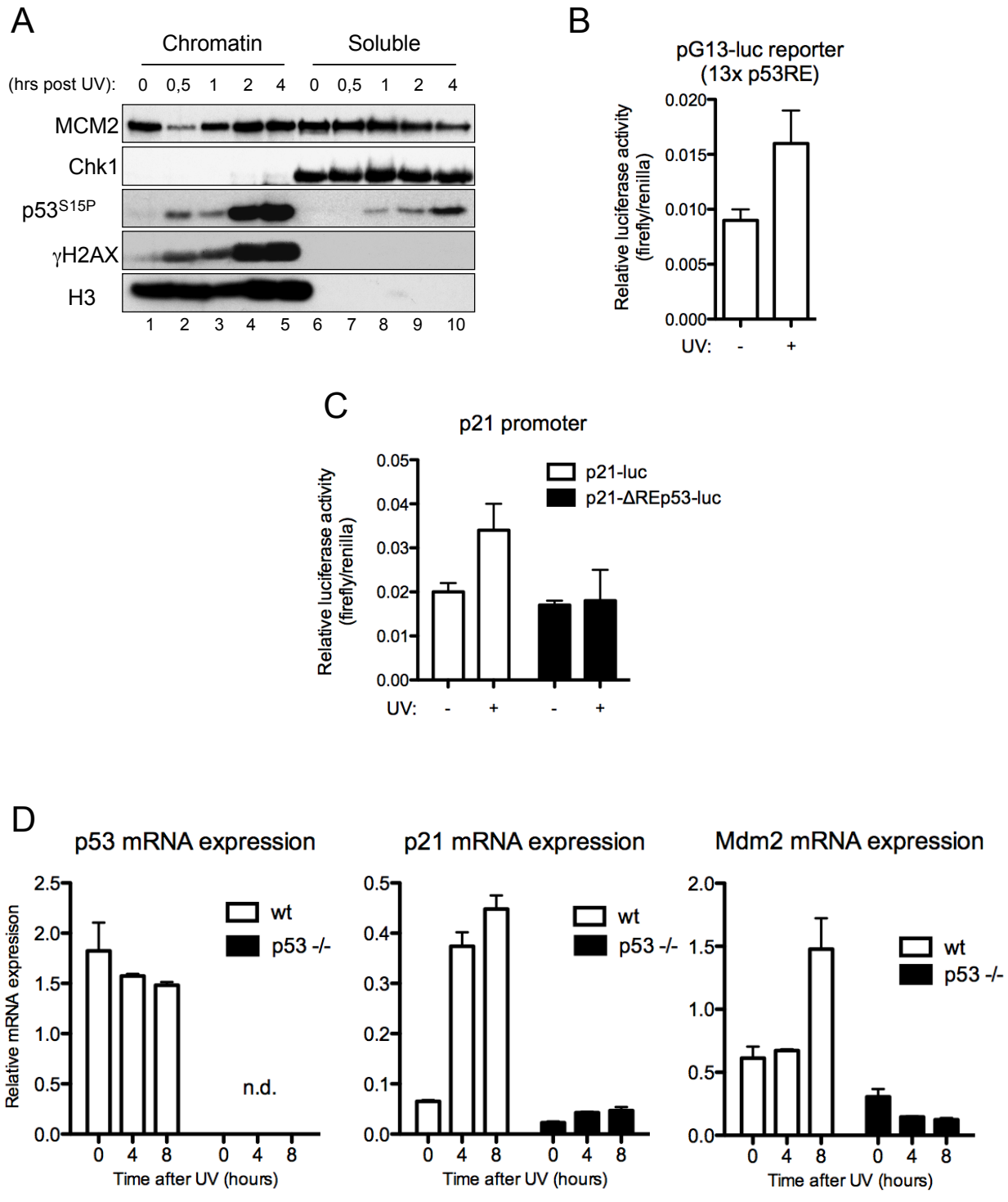
A
Chromatin
Soluble
(hrs post UV): 0 0,5 1 2 4 0 0,5 1 2 4
MCM2
Chk1
p53S15P
γH2AX
H3
1 2 3 4 5 6 7 8 9 10
B
pG13-luc reporter
(13x p53RE)
Relative luciferase activity
(firefly/renilla)
0.020
0.015
0.010
0.005
0.000
UV: - +
C
p21 promoter
p21-luc
p21-ΔREp53-luc
Relative luciferase activity
(firefly/renilla)
0.05
0.04
0.03
0.02
0.01
0.00
UV: - + - +
D
p53 mRNA expression
p21 mRNA expression
Mdm2 mRNA expression
wt
p53 -/-
Relative mRNA expresison
n.d.
Time after UV (hours)
0 4 8 0 4 8

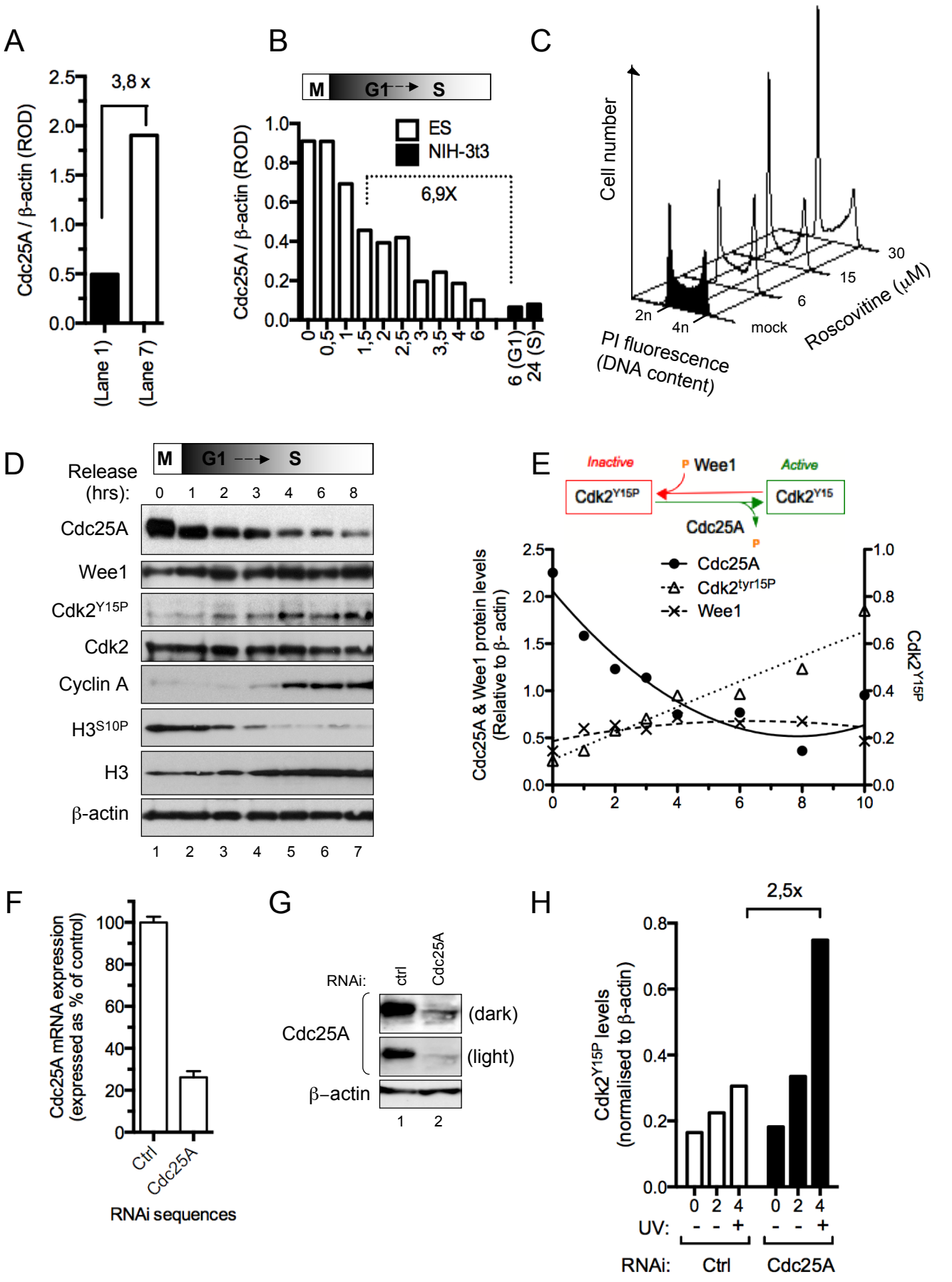
A
3,8 x
Cdc25A / β-actin (ROD)
(Lane 1)
(Lane 7)
B
M
G1
S
ES
NIH-3t3
6,9X
Cdc25A / β-actin (ROD)
6 (G1)
24 (S)
C
Cell number
PI fluorescence
(DNA content)
2n
4n
mock
6
15
30
Roscovitine (μM)
D
Release
(hrs):
0 1 2 3 4 6 8
Cdc25A
Wee1
Cdk2Y15P
Cdk2
Cyclin A
H3S10P
H3
β-actin
1 2 3 4 5 6 7
E
Inactive
P Wee1
Active
Cdk2Y15P
Cdk2Y15
Cdc25A
P
Cdc25A
Cdk2tyr15P
Wee1
Cdc25A & Wee1 protein levels
(Relative to β- actin)
Cdk2Y15P
F
Cdc25A mRNA expression
(expressed as % of control)
Ctrl
Cdc25A
RNAi sequences
G
RNAi:
ctrl
Cdc25A
Cdc25A
(dark)
(light)
β–actin
1 2
H
2,5x
Cdk2Y15P levels
(normalised to β-actin)
0 2 4 0 2 4
UV: - - + - - +
RNAi: Ctrl Cdc25A

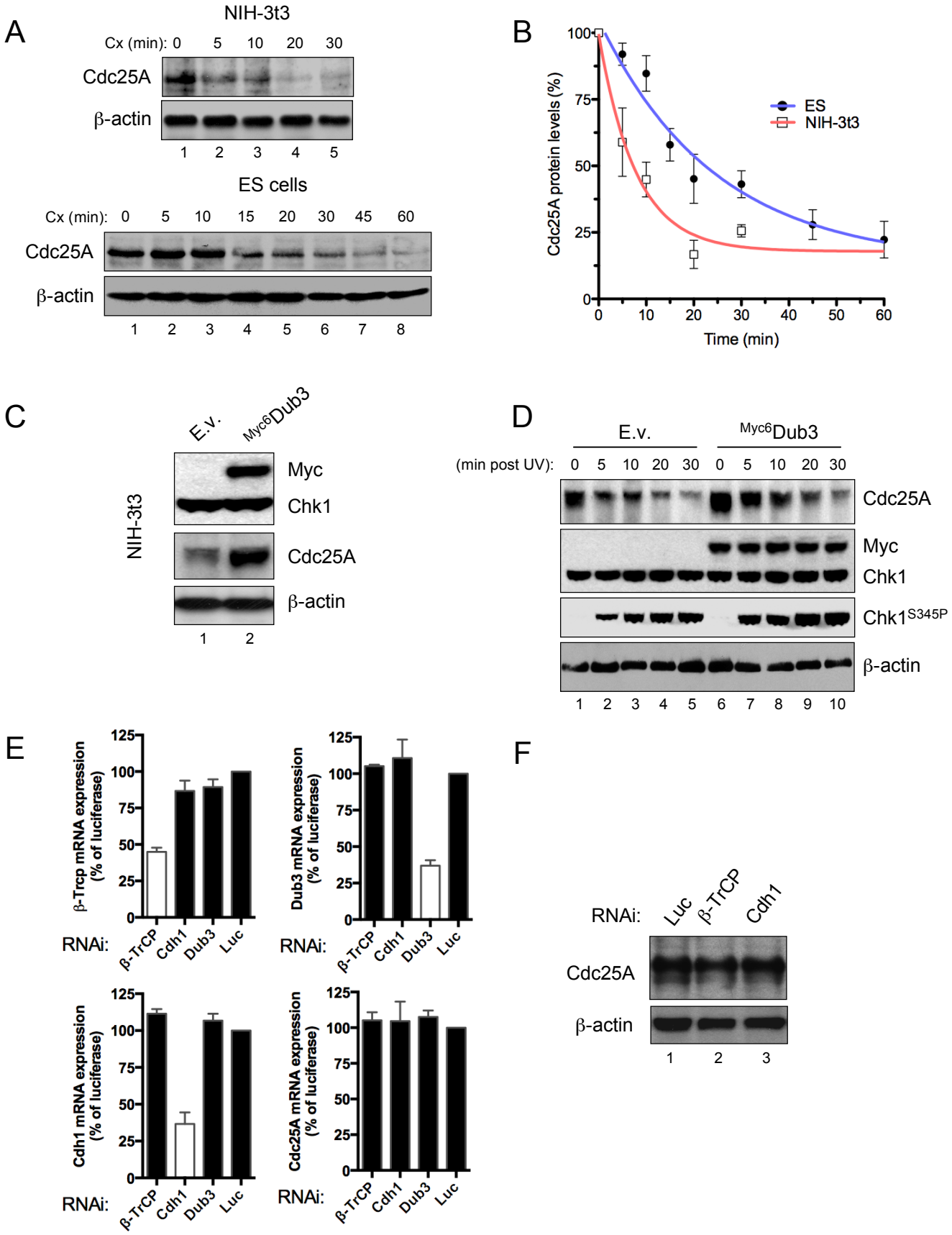
A
NIH-3t3
Cx (min): 0 5 10 20 30
Cdc25A
β-actin
1 2 3 4 5
ES cells
Cx (min): 0 5 10 15 20 30 45 60
Cdc25A
β-actin
1 2 3 4 5 6 7 8
B
Cdc25A protein levels (%)
100
75
50
25
0
0 10 20 30 40 50 60
Time (min)
ES
NIH-3t3
C
E.v.
Myc6Dub3
NIH-3t3
Myc
Chk1
Cdc25A
β-actin
1 2
D
E.v.
Myc6Dub3
(min post UV): 0 5 10 20 30 0 5 10 20 30
Cdc25A
Myc
Chk1
Chk1S345P
β-actin
1 2 3 4 5 6 7 8 9 10
E
β-Trcp mRNA expression (% of luciferase)
Dub3 mRNA expression (% of luciferase)
Cdh1 mRNA expression (% of luciferase)
Cdc25A mRNA expression (% of luciferase)
125
100
75
50
25
0
RNAi: β-TrCP Cdh1 Dub3 Luc
F
RNAi: Luc β-TrCP Cdh1
Cdc25A
β-actin
1 2 3

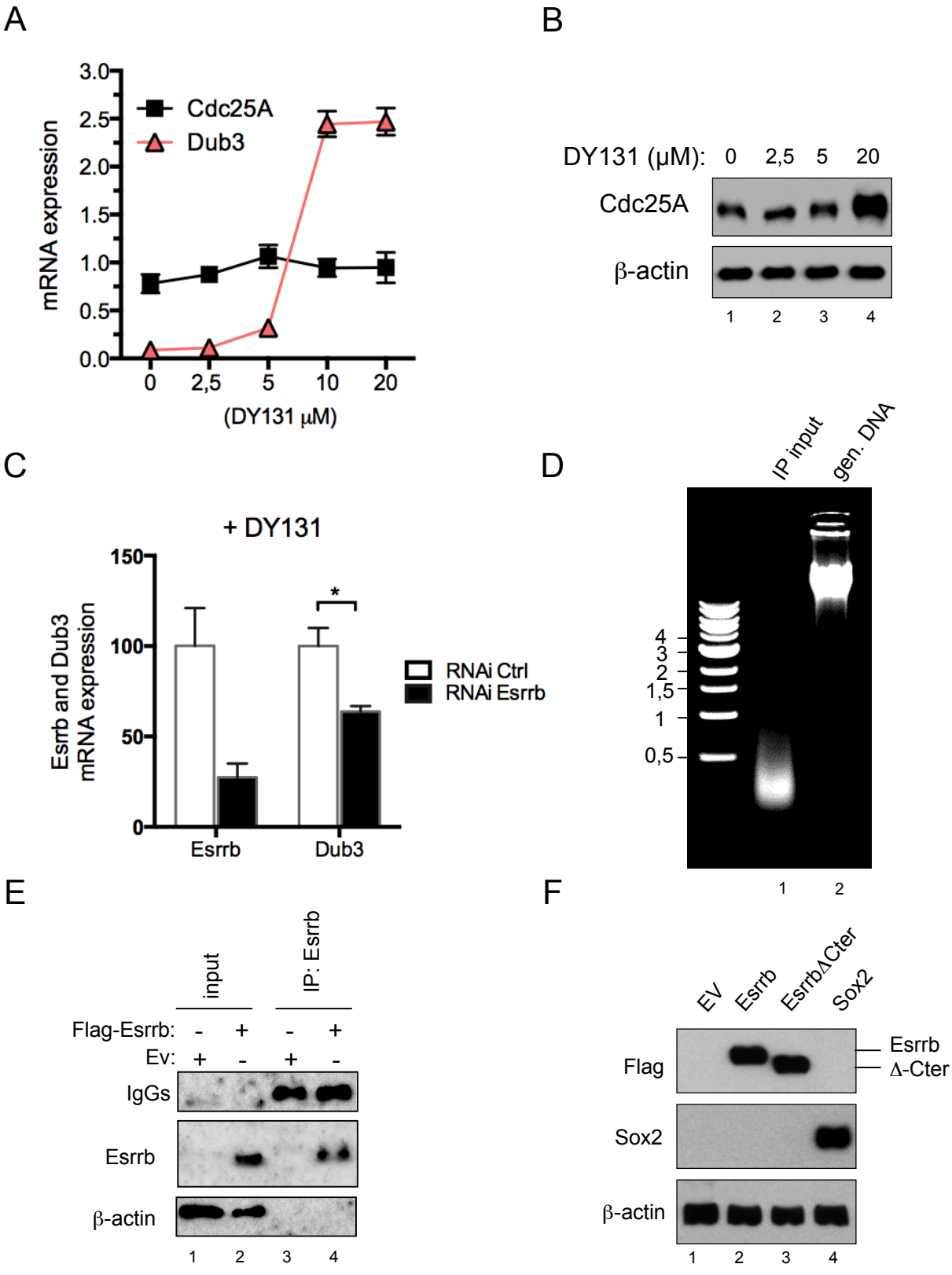
A
mRNA expression
3.0
2.5
2.0
1.5
1.0
0.5
0.0
Cdc25A
Dub3
0
2,5
5
10
20
(DY131 µM)
B
DY131 (µM): 0 2,5 5 20
Cdc25A
β-actin
1 2 3 4
C
+ DY131
Esrrb and Dub3 mRNA expression
150
100
50
0
*
RNAi Ctrl
RNAi Esrrb
Esrrb
Dub3
D
IP input
gen. DNA
4
3
2
1,5
1
0,5
1 2
E
input
IP: Esrrb
Flag-Esrrb: - + - +
Ev: + - + -
IgGs
Esrrb
β-actin
1 2 3 4
F
EV
Esrrb
EsrrbΔCter
Sox2
Flag
Esrrb
Δ-Cter
Sox2
β-actin
1 2 3 4

A

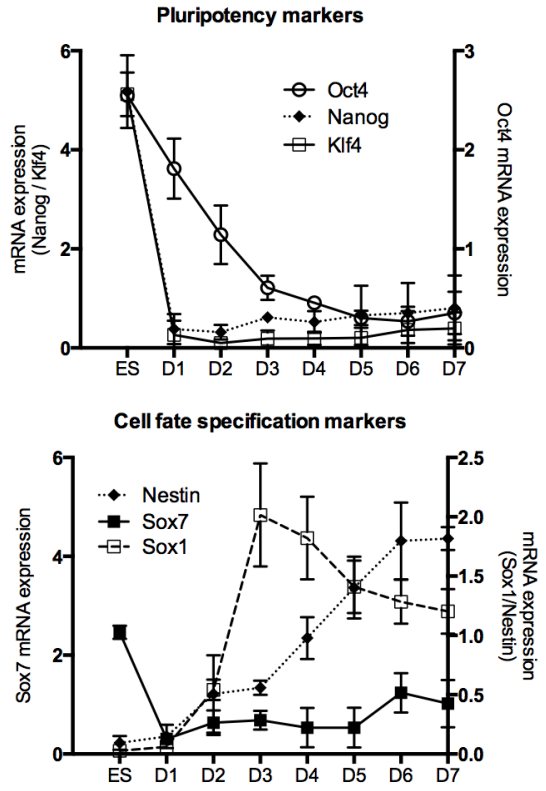
Pluripotency markers
mRNA expression (Nanog / Klf4)
Oct4 mRNA expression
Oct4
Nanog
Klf4
ES D1 D2 D3 D4 D5 D6 D7
Cell fate specification markers
Sox7 mRNA expression
mRNA expression (Sox1/Nestin)
Nestin
Sox7
Sox1
ES D1 D2 D3 D4 D5 D6 D7

B

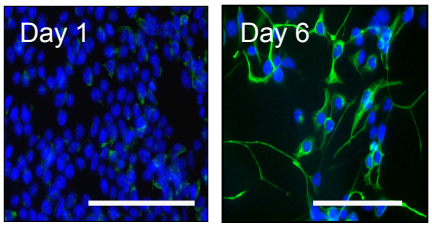
Day 1
Day 6

C

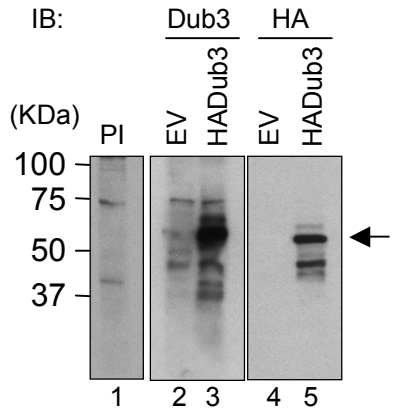
IB:
Dub3
HA
(KDa)
PI
EV
HADub3
EV
HADub3
100
75
50
37
1 2 3 4 5

D

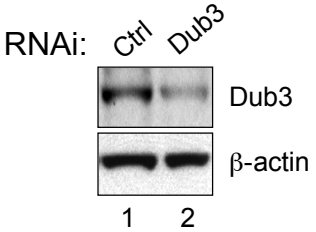
RNAi:
Ctrl
Dub3
Dub3
β-actin
1 2

E

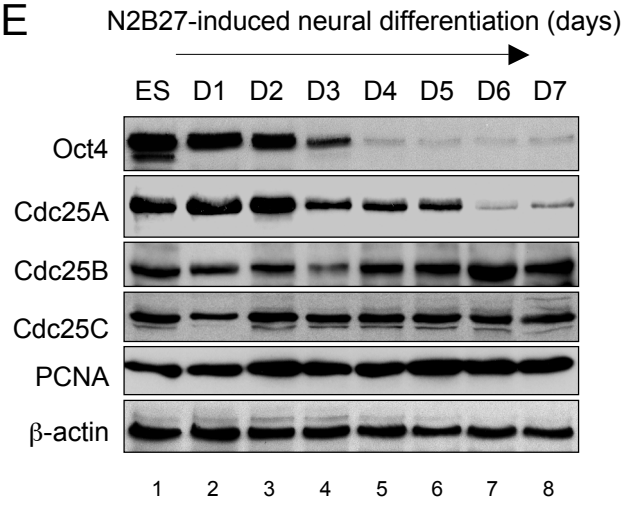
N2B27-induced neural differentiation (days)
ES D1 D2 D3 D4 D5 D6 D7
Oct4
Cdc25A
Cdc25B
Cdc25C
PCNA
β-actin
1 2 3 4 5 6 7 8

F

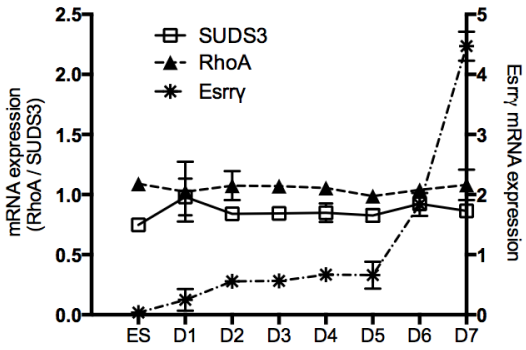
mRNA expression (RhoA / SUDS3)
Esrrγ mRNA expression
SUDS3
RhoA
Esrrγ
ES D1 D2 D3 D4 D5 D6 D7

G

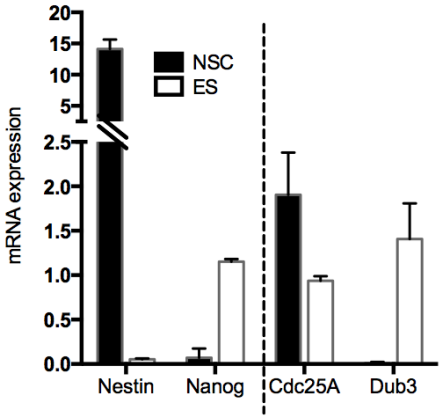
mRNA expression
NSC
ES
Nestin
Nanog
Cdc25A
Dub3

H

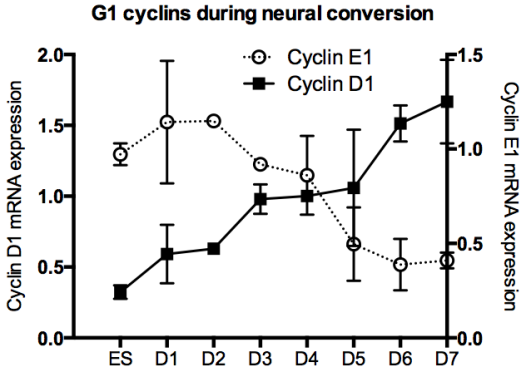
G1 cyclins during neural conversion
Cyclin D1 mRNA expression
Cyclin E1 mRNA expression
Cyclin E1
Cyclin D1
ES D1 D2 D3 D4 D5 D6 D7

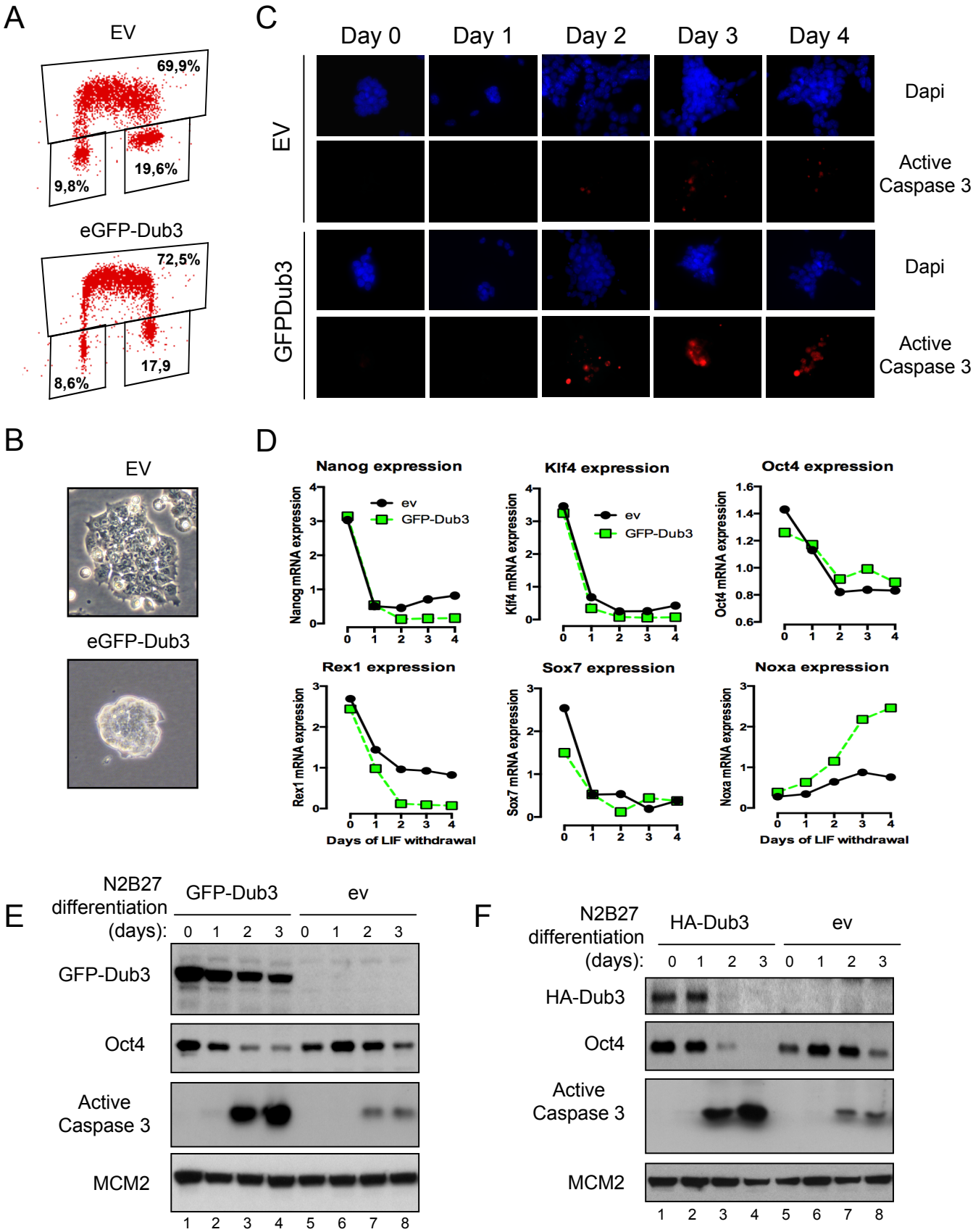
A
EV
69,9%
9,8%
19,6%
eGFP-Dub3
72,5%
8,6%
17,9
C
Day 0
Day 1
Day 2
Day 3
Day 4
EV
GFPDub3
Dapi
Active Caspase 3
Dapi
Active Caspase 3
B
EV
eGFP-Dub3
D
Nanog expression
Klf4 expression
Oct4 expression
Rex1 expression
Sox7 expression
Noxa expression
ev
GFP-Dub3
Nanog mRNA expression
Klf4 mRNA expression
Oct4 mRNA expression
Rex1 mRNA expression
Sox7 mRNA expression
Noxa mRNA expression
Days of LIF withdrawal
Days of LIF withdrawal
E
N2B27 differentiation (days):
GFP-Dub3
ev
0 1 2 3 0 1 2 3
GFP-Dub3
Oct4
Active Caspase 3
MCM2
1 2 3 4 5 6 7 8
F
N2B27 differentiation (days):
HA-Dub3
ev
0 1 2 3 0 1 2 3
HA-Dub3
Oct4
Active Caspase 3
MCM2
1 2 3 4 5 6 7 8

Supplemental Information

High Dub3 expression in mouse ES cells couples the G1/S checkpoint to pluripotency

Siem VAN DER LAAN, Nikolay TSANOV, Carole CROZET and Domenico MAIORANO

Supplemental Figure legends

Figure S1 (related to Figure 1): DNA damage in G1 induces transient cell cycle arrest in early S-phase and not at the G1/S transition.

(A) UV-dependent cell cycle changes of ES Cells. Cell cycle profile of asynchronously growing ES cells exposed to increasing dose of UV-light (2-10 J/m^2). Cells were collected 6 hours after UV-irradiation for FACS analysis.

(B) Cell cycle profile of UV-exposed ES cells in time. Asynchronously growing ES cells were exposed to 6 J/m^2 UV-irradiation and collected for FACS analysis at indicated time points.

(C) Immunofluorescence detection of Oct4 in ES and NIH-3t3 cells. Nuclei were counterstained using DAPI. Scale bar 10 μM.

(D) Subcellular fractionation of ES cells released from nocodazole arrest, mock or UV-irradiated in G1 (2 hours after release) collected at indicated time points. Cells were lysed and fractionated into soluble and insoluble (chromatin-bound) fraction as described in Materials and methods.

(E) qPCR quantification of Cyclin E1 and Cyclin A2 mRNA normalised to multiple reference genes from ES cells released from nocodazole arrest mock or UV-irradiated in G1 and collected at indicated time points. Dotted line represents levels in G1. Data are expressed as mean ± SD (error bars) of multiple observations.

Figure S2 (related to Figure 1): p53 is transcriptionally active in ES cells upon DNA damage.

(A) Subcellular fractionation of ES cells UV-irradiated and collected at indicated time points. Cells were lysed and fractionated into soluble and insoluble (chromatin-bound) fraction as described in Materials and methods.

(B) ES cells transfected with pG13-luc promoter (containing p53 response elements) were mock or UV-irradiated and processed for luciferase activity. Bars represent the mean ± SD of triplicate observations.

(C) ES cells transfected with p21-luc and p21-ΔREp53-luc (lacking p53 response element) were mock or UV-irradiated and processed for luciferase activity. Bars represent the mean ± SD of triplicate observations.

(D) qPCR quantification of p53, p21 and Mdm2 mRNA normalised to multiple reference genes. Wild-type (wt) and p53 knockout ($p53^{-/-}$) ES cells were UV-irradiated and collected at indicated time points for analysis of mRNA expression of main p53 target genes. Bars represent the mean ± SD of triplicate observations.

Figure S3 (related to Figure 2): Persistent Cdc25A phosphatase upon DNA damage in G1 inhibits G1/S checkpoint in ES cells.

(A) Quantification of western blotting signals shown in Fig. 2A Western blot signals (lane 1 and lane 7) of Cdc25A (dark exposure) were quantified by densitometry scanning and expressed as relative optical density (ROD) compared to β-actin signal as loading control.

(B) Quantification of western blotting signals shown in Figure 2B. Western blot signals of Cdc25A were quantified by densitometry scanning and expressed as relative optical density (ROD) compared to β-actin signal as loading control.

(C) Roscovitine, a potent and selective inhibitor of cyclin-dependent kinases, dependent lengthening of the G1 phase of ES cells. FACS analysis of asynchronously growing ES cells treated with increasing concentration of Roscovitine.

(D) Cdk2 phosphorylation status (Y15P) during an unperturbed cell cycle. ES cells were released from nocodazole arrest and collected in G1 and S-phase at indicated time points. Proteins were detected with the indicated specific antibodies by western blotting.

(E) Schematic representation of the regulation of phosphorylation on Cdk2 by Wee1 and Cdc25A. Western blot signals of panel (C) were quantified by densitometry scanning and expressed as relative optical density (ROD) compared to β-actin signal as loading control.

(F) qPCR quantification of Cdc25A mRNA normalized to multiple reference genes expressed as percentage of control. ES cells were transfected with control (Crtl) RNAi or Cdc25A RNAi sequences. Bars represent the mean ± SD of multiple observations.

(G) Western blot analysis of ES cells transfected with control (Crtl) or Cdc25A RNAi sequences.

(H) Quantification of western blotting signals shown in Figure 2E. Western blot signals of Fig. 2E were quantified by densitometry scanning and expressed as relative optical density (ROD) compared to Chk1 signal as loading control.

Figure S4 (related to Figure 3): Elevated deubiquitylating enzyme Dub3 in ES cells results in Cdc25A abundance.

(A) Representative western blot signal used for determination of Cdc25A turnover rate in the presence of cycloheximide (Cx) in ES and NIH-3t3 cells. Cells were collected at indicated time points.

(B) Cdc25A turnover rate in the presence of cycloheximide (Cx) in ES and NIH-3t3 cells. Western blot signals of Cdc25A were quantified by densitometry scanning and expressed as relative optical density (ROD) compared to β-actin signal as loading control. Signal in untreated cells were set at 100% and half-life ($t_{1/2}$) of Cdc25A was determined (data are represented as mean ± SD).

(C) Overexpression of Dub3 increases Cdc25A abundance. NIH-3t3 cells were transduced with empty vector (E.v.) or pLPC encoding Myc_6-Dub3. After puromycin selection cells were collected and processed for western blot analysis.

(D) Cdc25A degradation upon DNA damage in NIH-3t3 cells expressing empty vector (E.v.) or pLPC encoding Myc_6-Dub3. Cells were collected at indicated time points and analyzed by western blotting.

(E) qPCR quantification of indicated mRNA normalised to multiple reference genes expressed as percentage of control. ES cells were transfected with control (Luc), β-TrCP, Cdh1 or Dub3 RNAi sequences and collected 48 hours after transfection. Bars represent the mean ± SD of triplicate observations.

(F) Western blot analysis of Cdc25A protein in RNAi-transfected cells.

Figure S5 (related to Figure 4): Dub3 is a target gene of the orphan receptor Esrrb

(A) qPCR quantification of Cdc25A and Dub3 mRNA in ES cells treated with increasing concentration of the selective Esrrb and Esrrg agonist DY131 for 16 hours. Bars represent the fold induction ± SD of triplicate observations.

(B) Western blot analysis of Cdc25A protein levels in ES cells treated with increasing concentration of the DY131agonist for 16 hours.

(C) qPCR quantification of Esrrb and Dub3 mRNA normalised to multiple reference genes expressed as percentage of control in presence of DY131. ES cells were transfected with control (Crtl) RNAi (white bars) or Esrrb specific RNAi sequence (black bars). Data are expressed as mean ± SD (error bars) of multiple observations.

(D) DNA fragments size prior to ChIP analysis. Sonication resulted to DNA fragments smaller than 500bp.

(E) Specificity of the Esrrb antibody. Immunoprecipitation of 293T-HEK cells transfected with either empty vector (Ev) or Flag-Esrrb expression plasmids. Immunoprecipitation was performed in parallel using either Flag or Esrrb antibody. Both antibodies specifically immunopreciptated Flag-Esrrb protein.

(F) Western blot analysis of expression levels of CV1 cells transfected with either empty vector (lane 1), Flag-Esrrb (lane 2), Flag-Esrrb Δ-Cter (lane 3) or Sox2 (lane 4), 48 hours post-transfection.

Figure S6 (related to Figure 5): Developmental regulation of Cdc25A protein abundance correlates with Dub3 expression levels.

(A) qPCR quantification of pluripotency and cell fate specification markers during neural conversion of ES cells. Data were normalized to multiple reference genes. Data are expressed as mean ± SD (error bars) of multiple observations.

(B) Immunofluorescence detection of Nestin at day 1 and day 6 of N2B27-induced differentiation. Nuclei were counterstained using DAPI. Scale bar 50 μM.

(C) Specificity of the antibody raised against mouse Dub3. Human 293T cells were transfected with empty vector (EV) or HA-Dub3 expressing vectors. Cells were collected 24 hours post transfection and extracts were immunoblotted (IB) using pre-immune (PI), Dub3 or HA antibodies. The Dub3 antibody recognizes a specific polypeptide of 60 kDa in SDS-PAGE (arrow) which is not recognized by the pre-immune serum.

(D) Validation of the antibody raised against mouse Dub3. Western blot analysis of ES cells transfected with control (lane 1) or Dub3 (lane 2) RNAi sequences. Cells were collected 48 hours post transfection and extracts were immunoblotted using Dub3 purified antibody and β-actin.

(E) Western blot analysis of Dub3 substrates and indicated proteins during neural conversion.

(F) qPCR quantification of Suds3, RhoA and Esrr g during neural conversion of ES cells. Data were normalized to multiple reference genes. Data are expressed as mean ± SD (error bars) of multiple observations.

(G) qPCR quantification of Nestin, Nanog, Cdc25A and Dub3 mRNA normalized to multiple reference genes in ES and Neural Stem Cells (NSC). Bars represent the mean ± SD of multiple observations.

(H) qPCR quantification of G1 cyclin stoechiometry during neural conversion of ES cells. Data were normalised to multiple reference genes. Data are expressed as mean ± SD (error bars) of multiple observations.

Figure S7 (related to Figure 6): Constitutive Dub3 expression leads to massive apoptosis concomitant to differentiation-induced cell cycle remodeling.

(A) Cell cycle distribution and BrdU incorporation of empty vector (EV) and eGFP-Dub3 expressing ES cells analysed by FACS.

(B) Phase contrast photos of eGFP-Dub3 and EV expressing cell-lines.

(C) Immunoflorescnece detection of active capsase 3 during LIF withdrawal in empty vector and eGFP-Dub3 expressing ES cells.

(D) qPCR quantification of pluripotency markers (Nanog, Klf4, Oct4, Rex1), of Sox7 and of Noxa normalised to multiple reference genes during LIF withdrawal.

(E) Western blot analysis of cell extracts collected every day throughout the N2B27-induced differentiation process of empty vector or eGFP-Dub3 expressing ES cells into NSCs. Of note, four days after N2B27-mediated differentiation all eGFP-Dub3 expressing cells were all dead by apoptosis as indicated by high caspase 3 activities.

(F) Western blot analysis of cell extracts collected every day throughout the differentiation process of empty vector or HA-Dub3 expressing ES cells into NSCs. The molecular and cellular phenotype of HA-Dub3 expressing cells was highly

comparable to the eGFP-Dub3 expressing cells indicating that the phenotype is independent of the N-terminal tag.

Supplemental Experimental Procedures

Cell culture and transfection

Briefly, ES cells were maintained in Glasgow MEM BHK-21 (GMEM) supplemented with 10% fetal bovine serum, non-essential amino acids, L-glutamine, sodium pyruvate, β-mercapthethanol. NIH-3t3 cells were maintained in Dulbecco's modified eagle's medium (DMEM) supplemented with 10% fetal bovine serum, 2 mM glutamine and antibiotics. The viruses-containing conditioned medium was incubated on exponentially growing NIH-3t3 cells for 24 hours in the presence of polybrene (10 mg/mL). 48 hours post-infection, cells were selected in puromycin (2.5 μg/mL)-containing medium for 8-10 days before use. Reverse transfection of ES cells was performed using INTERFERin (Polyplus) according to manufacturer's directions. Cells were collected 24, 36 or 48 hours after transfection for analysis. The Cdc25A RNAi sequence was 5'-GAAAUUUCCCUGACGAGAA-3', Dub3 5'-GGCUGUAAGAUGUGUGCUA-3' and a Esrrb previously described (Feng et al., 2009). RNAi for Cdh1 and β-TrCP knockdown were purchased from Darmacon (SMARTpool) 57371 (Cdh1) and 12234 (β-TrCP).

Monolayer differentiation of ES cells into neurectodermal precursors.

ES cells were dissociated and plated in N2B27 medium onto 0.1% gelatine-coated dishes at a density of 1.10^4 cells/cm². N2B27 medium is a 1:1 mixture of DMEM/F12 (Gibco) supplemented with modified N2 (25 μg/ml insulin, 100 μg/ml apo-transferrin, 6 ng/ml progesterone (Sigma), 16 μg/ml putrescine (Sigma), 30 nM sodium selenite (Sigma), 50 μg/ml bovine serum albumine (Gibco), Neurobasal medium supplemeted

with B27 (Gibco), β-mercaptoethanol (0.1 mM) and glutamate (0.2 mM) was also added. The medium was replaced every two days until day 7.

Plasmids

The murine Dub3 gene (Gene ID: 625530) was amplified by PCR and cloned into pLPC-Myc_6, pcDNA3-GFP and pcDNA3-HA. All constructs were verified by DNA sequencing. Mouse Esrrb (pSG5FI-mEsrrb) and the C-terminal truncated pSG5FI-mEsrrb-ΔCter were previously described (Vanacker et al., 1999). Genomic sequences of the Dub3 promoter were amplified by PCR and inserted into pGL4.10 vector (Promega) for luciferase activity. pCEP4-Sox2 was a kind gift of F. Poulat (IGH-CNRS).

Cell extracts, western blotting and antibodies

Cells were rinsed once in PBS and then incubated with ice cold lysis buffer (50 mM Tris-HCl pH 7.4, 100 mM NaCl, 50 mM NaF, 5 mM EDTA, 40 mM β-glycero-phosphate, 1% Triton X-100 and protease inhibitors) for 30 min on ice before scraping. Whole cell extracts were clarified by centrifugation at 12000 rcf for 10 min at 4°C. Protein concentration of the clarified lysates was estimated using BCA method (Pierce). Equal amount of protein was used for western blot analysis. All antibodies were incubated overnight at 4 °C in phosphate-buffered saline (PBS) containing 1% BSA and 0,1% Tween (Sigma). Antibodies used from Cell Signaling: $Chk1^{S345P}$ (2341), $p53^{S15P}$ (9284), γH2AX (2577), $CDK2^{Y15P}$ (9111), Myc-Tag (2276); active caspase 3 (9961); $p53^{S15P}$ (9284), γH2AX (2577); Active caspase 3 (9961);

Abcam: DNA polα(ab31777), H3 (ab1791), CDK2 (ab6538), PSTAIR (ab10345), GFP (ab290), DNA polα(ab31777), H3 (ab1791), MCM2 (ab4461); Suds3 (ab3740) Santa Cruz: Cdc45 (sc-20685), Cdc25A (sc-7389), Chk1 (sc-8408), Cyclin B1 (sc-245), Cdc25C (sc-327), Cdc25B (sc-65504), p21 (sc-6246), Cdc45 (sc-20685), Cdc25A (sc-7389), Chk1 (sc-8408); RhoA (sc-418); anti-goat IgG-HRP (sc-2020) Sigma: (PC10), β-actin (A1978), Cyclin A (C7410), Anti-Flag M2 (F1804), β-actin (A1978), Cyclin A (C7410), Flag (F3165); Oct4 (Chemicon, AB3209), and Millipore, Nestin (Ab353), $H3^{S10P}$ (Millipore 09-797). Wee1 (kindly provided by T. Lorca, CRBM Montpellier).

Mouse Dub3 polyclonal antibodies were raised by immunizing rabbits with a synthetic peptide (NH2-MSPGQLCSQGGR-COOH) designed from mouse Dub3 C-terminus, coupled to keyhole limpet hemocyanin (KLH). Antibodies were purified by coupling the Dub3 peptide on HiTrap NHS-activated HP columns (GE Healthcare).

Chromatin immunoprecipitation

Cells were lysed in ice-cold lysis buffer (50 mM Tris-HCl pH 7.4, 100 mM NaCl, 50 mM NaF, 5 mM EDTA, 40 mM β-glycero-phosphate, 1% SDS, 1% Triton X-100 and protease inhibitors) for 30 min on ice. Immuoprecipitation was performed by adding 5 μg Esrrb (Sigma SAB2100715), Sox2 (Bethyl A301-739) or control antibodies (Peprotech 500-P00) to lysates and incubation with rotation overnight at 4 °C. BSA and salmon sperm-blocked Protein A-Sepharose (Amersham) beads were added to the lysate.

Luciferase assay

ES cells were transfected with following reporter constructs, pG13-luciferase, p21-luciferase and p21-ΔREp53-luc (kindly provided by J. Basbous, IGH, Montpellier). A

Renilla luciferase plasmid was cotransfected as an internal control. Cells were harvested 24 hours after transfection and mock or UV-irradiated. Six hours following UV-induced DNA damage, cells were harvested and the luciferase activities of the cell lysates were measured using the Dual-luciferase Reporter Assay system (Promega). The proximal promoter of 1kb upstream ATG start codon was inserted into pGL4.10 plasmid. Three mutations of the Esrrb consensus binding site (TCAAGGTCA) were introduced by PCR to generate a mutated binding site (TCATTTTCA). All constructs were sequence verified.

Immunofluorescence microscopy

For Nestin, Oct4 and active caspase 3 staining staining, cells were fixed in 4% paraformaldehyde and permeabilized with 0,1% Triton X-100. After fixation, cells were blocked in 3% BSA PBS-Tween and incubated overnight with antibody. The slides were mounted using Prolong Gold with DAPI (Invitrogen). For determination of the cellular localisation of Dub3, mouse ES cells were transfected with pcDNA-GFP-Dub3 and directly fixed. All slides were analysed using a Leica DM6000 epifluorescence microscope. Images were acquired using a Coolsnap HQ CCD camera (Photometrics) and the metamorph software (Molecular Devices).

Subcellular fractionation experiments

Chromatin-enriched and soluble fractions were prepared using CSK-extraction procedure. Briefly, pelleted cells were lysed in CSK buffer (10 mM PIPES pH 6.8, 100 mM NaCl, 300 mM sucrose, 1 mM EGTA, 1 mM $MgCl_2$, 0.5 mM DTT, 1 mM ATP, 0.2% Triton X-100 and protease inhibitors) for 10 min on ice. After centrifugation at

3000 rpm for 3 min at 4 °C, the supernatant (Triton-soluble fraction) was recovered and the pellet (Triton-insoluble fraction) was resuspended in CSK buffer and incubated for 10 min on ice. After centrifugation, the pellet (chromatin-enriched fraction) was resuspended in Laemmli Buffer. Equivalent amount of soluble and chromatin fractions were analyzed by immunoblotting.

Statistical analysis

Two-way ANOVA or Student t-test were used to evaluate differences between groups using Prism software (GraphPad Software). $P < 0.05$ was considered significant and indicated with *, $P < 0.001$ was indicated with **.